November 2016

Multi-Classifier Fusion Strategy for Activity and Intent Recognition of Torso Movements

Abhijit Kadrolkar

MULTI-CLASSIFIER FUSION STRATEGY FOR ACTIVITY AND INTENT RECOGNITION OF TORSO MOVEMENTS

A Dissertation Presented

by

ABHIJIT KADROLKAR

Submitted to the Graduate School of the
University of Massachusetts Amherst in partial fulfillment
of the requirements for the degree of

DOCTOR OF PHILOSOPHY

September 2016

Department of Mechanical and Industrial Engineering

MULTI-CLASSIFIER FUSION STRATEGY FOR ACTIVITY AND INTENT RECOGNITION OF TORSO MOVEMENTS

A Dissertation Presented

by

ABHIJIT KADROLKAR

Approved as to style and content by:

_____
Frank C. Sup IV, Chair

_____
Yossi Chait, Member

_____
Kourosh Danai, Member

_____
Brian R. Umberger, Member

_____
Sundar Krishnamurty, Department Head
Department of Mechanical and Industrial Engineering

DEDICATION

To my grandparents, Nana and Tai.

ACKNOWLEDGMENTS

I would like to thank my advisor Prof. Frank Sup, for his insightful and patient, guidance, support and encouragement for all these years that I have been working with him. His depth of knowledge and ability to glean insights from very little information have been very helpful in me completing this dissertation. I would also like to extend my gratitude to the members of my dissertation committee, Prof. Yossi Chait, Prof. Kourosh Danai and Prof. Brian Umberger, for their invaluable advice and feedback.

All the data used in this dissertation was collected in the Biomechanics Lab, and I will be forever grateful to Prof. Brian Umberger and his colleagues at the Biomechanics Lab, for extending to me the use of his lab and equipment. Also, thanks to Dr. Ulvi Baspinar for being a steady and insightful collaborator.

Working at MRRL has been a very special time and I would like to extend my appreciation to all the members of MRRL who have made this journey fun, interesting and worthwhile. During the time I spent in the Amherst area, I have been fortunate to have formed a small number of very close friendships, and I would like to extend a heartfelt thank you to all my friends.

I would be remiss if I didn't mention my gratitude to my parents, who have been unflinching in their love, support and encouragement. Throughout my time in grad school, my parents were a constant, unwavering source of encouragement. Their love and steadfast support has been immensely instrumental to the completion of this dissertation, and for this I am eternally grateful.

ABSTRACT

MULTI-CLASSIFIER FUSION STRATEGY FOR ACTIVITY AND INTENT RECOGNITION OF TORSO MOVEMENTS

SEPTEMBER 2016

ABHIJIT KADROLKAR,

B.E., VISVESWARAYA TECHNOLOGICAL UNIVERSITY, INDIA

M.S., UNIVERSITY OF MASSACHUSETTS AMHERST

Ph.D., UNIVERSITY OF MASSACHUSETTS AMHERST

Directed by: Professor Frank C. Sup IV

As assistive, wearable robotic devices are being developed to physically assist their users, it has become crucial to develop safe, reliable methods to coordinate the device with the intentions and motions of the wearer. This dissertation investigates the recognition of user intent during flexion and extension of the human torso in the sagittal plane to be used for control of an assistive exoskeleton for the human torso. A multi-sensor intent recognition approach is developed that combines information from surface electromyogram (sEMG) signals from the user's muscles and inertial sensors mounted on the user's body. Intent recognition is implemented by following a pattern classification approach, wherein a linear discriminant analysis (LDA) based method of pattern classification is utilized. This method of classification builds on a traditional LDA by utilizing multiple classifiers from multiple sensors that are combined together using a majority voting based classifier fusion scheme, to deliver improved classification performance. Additionally, there is a focus on identification of suitable features for

classification. Extraction of features in the time, frequency and time-frequency domains is discussed. Wavelet transform methods are employed for targeted extraction of nonlinear time-frequency domain features, and the effectiveness of these features in improving classification performance is emphasized. Experimental results using sEMG and inertial signals recorded from human subjects, to evaluate the pattern classification and feature extraction methods are presented. Results show that a combined sensor approach that utilizes both inertial and sEMG data leads to a 70% improvement in classification performance. Results also show that the use of multiple time-frequency domain features in conjunction with majority voting based classifier-fusion leads to an additional 75% improvement in classification performance, with a best case of up to 97% accuracy in recognizing user intent. This research has provided an effective demonstration of leveraging nonlinear time-frequency domain features with linear methods of classification to deliver accurate and computationally efficient intent recognition. In addition, the research effort has also developed a library of features that can serve as a starting point for future efforts in classifying torso motions.

TABLE OF CONTENTS

Page

LIST OF TABLES

Table Page

LIST OF FIGURES

Figure Page

CHAPTER 1

INTRODUCTION

Intent recognition, and recognition of activities and motions performed is an open research problem in the field of bio-robotics, wearable sensing, robotic prostheses and assistive devices [1]–[3]. In such applications, intent recognition is usually driven by physiological sensor measurements recorded from the user's body [4], [5]. The problem of recognizing intent from physiological sensor data becomes problems of extraction, identification and classification of patterns occurring in the sensor data [6].

Machine learning based methods of pattern classification are among the most useful tools available for addressing such problems. The available methods of pattern classification can be broadly classified into linear and non-linear methods [7]. Linear methods are generally preferable owing to their inherent computational efficiency, ease of implementation, relative insusceptibility to overfitting, and reduced sensitivity to noise. However, the need to extract and classify complex spatial and temporal patterns from noisy, multidimensional time-series data obtained from physiological measurements cannot be easily satisfied by linear methods. On the other hand, non-linear methods, although powerful in extracting and classifying complex patterns have inherent issues related to computational complexity, susceptibility to overfitting, and sensitivity to noise [8].

This dissertation explores the combination of these two domains by utilizing non-linear features in conjunction with linear methods of classification, in order to obtain classification accuracy that is similar to that of non-linear methods, without being subject

to the negative aspects of non-linear classification. As part of this exploration this dissertation investigates methods of feature extraction suitable for representing complex spatial and temporal patterns in time-series data, and methods for combining these features with simple, linear methods of classification.

The abovementioned exploration is carried out by studying a representative problem of intent recognition of human torso movements. The study of intent recognition of torso movements finds applicability in assistive devices for the upper body, and is a currently nascent field of research.

1.1 Motivation

The study of an intent recognition system for torso movements is motivated in part by the need for a safe, efficient, and reliable control and interface system for a powered, assistive device for the back and upper body. The design of such a device was introduced by the author and colleagues in a previous publication, and research on realizing the device is ongoing [9]. The device is intended to provide strength augmentation and injury protection to healthy users, to help carry heavy loads. In addition, the device is also intended to have healthcare applications, such as restoring mobility and motion after stroke or spinal cord injury.

The emphasis on linear methods of classification is driven by the need for a computationally efficient real-time implementation of the method of intent recognition, and the drive to explore non-linear features is motivated by the need for achieving linear separability in the feature space so that linear methods of classification would be sufficiently effective.

1.2 Review of Literature

1.2.1 Actuation of Torso Motion

All human motion is the result of biomechanical interactions between muscles, the skeletal frame and the environment, with muscles being the primary actuators [10]. Muscular actuation of the torso is achieved by a combination of 'local' and 'global' muscles [10]. The global muscles perform gross motions like controlling the overall posture, and transferring loads from the thoracic cage to the spine and from the spine to the pelvis [10]–[12]. The global muscles include the erector spinae, the obliques and abdominal muscles [10], [13]. The local muscles control the stiffness and curvature of individual spine segments [12], [14], [15]. The prominent muscles that make up the set of local muscles are the interspinal, intertransverse and multifidus muscles [10], [13]. In addition to being part of a biomechanical system that causes motion, muscles are also part of an electrical system that comprises of the central nervous system (CNS) of the body. The electrical activity of this electrical system can be measured as a voltage. This voltage measurement is called an electromyogram, and provides a measure of the intent for locomotion [16].

1.2.2 Electromyography (EMG)

An electromyogram (EMG) is a recording of the electrical activity in a muscle. In the case of muscles that are attached to the skeleton and are primary actuators during locomotion, it contains information about the neural control of the underlying musculature. This is due to the fact that human intent for locomotion is communicated to the muscles through electrical transmissions generated by the central nervous system (CNS).

Transmissions from the CNS to muscles and other end effectors are carried by transient electrical impulses that begin in neurons and propagate towards their target cells at velocities between 0.3 m/s and 100 m/s [17]. Muscular actuation happens at the cellular level due to the relative motion between actin and myosin filaments. Repeating ordered arrangements of these filaments form a myofibril. A network of such myofibrils forms a muscle fiber, which is a multi-nucleated cell. These muscle fibers are bundled to form fascicles and bundles of these fascicles form a complete muscle. A graphical representation of this muscular organization is shown in Fig. 1.1.

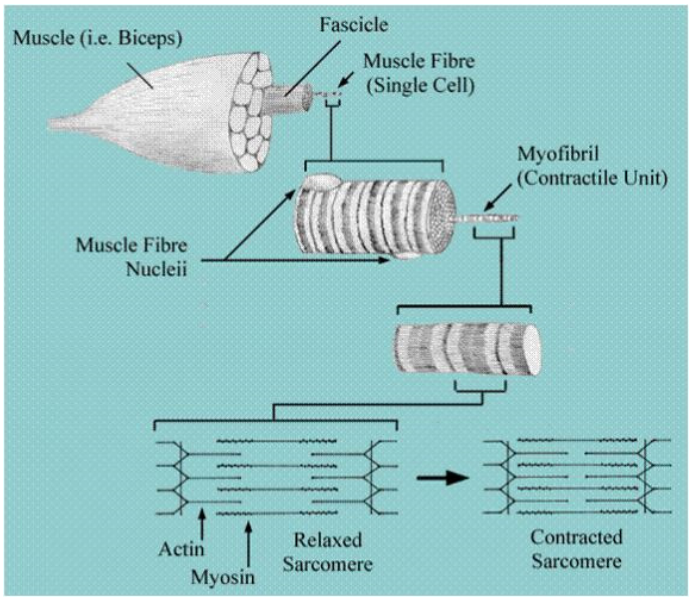

Figure 1.1: Structural organization of muscle [10].

The muscle fiber is the structural unit of a muscle. A group of muscle fibers is controlled (innervated) by a single neuron, called a motoneuron. These muscle fibers are connected to the motoneuron via motor axons and this assembly of a motoneuron, the motor axon, and the muscle fibers innervated by that neuron is called a motor unit [10], [17]. A motor unit is the functional unit of a muscle and is the primary unit of control in

the neuromuscular system [16]. As can be seen in the motor unit in Fig. 1.2, multiple muscle fibers are innervated by a single motoneuron. Therefore, the firing of a single motoneuron results in multiple muscle fibers discharging almost simultaneously. The aggregate activity of all these muscle fibers results in the generation of a motor unit action potential, which can be recorded by EMG [13], [16].

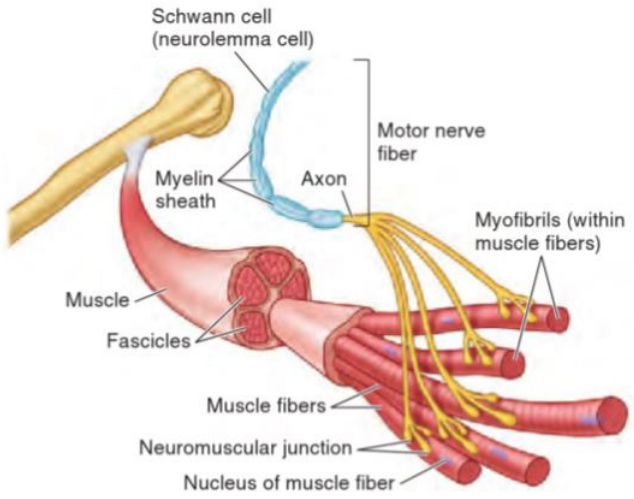

Figure 1.2: Motor Unit: Motoneuron, motor axon, muscle fibers [10].

Movement and muscular force output is a result of the activation of motor units. The central nervous system responds to the requirement for additional force either by activating additional motor units or by increasing the frequency of activation of motor units. The motor units to be activated are selected (or recruited) in increasing order of size, with the smallest motor units being recruited first and larger motor units recruited according to force requirements. The choice of motor units and their rates and times of discharge are made by the central nervous system, based on the extant intention [17].

This motor unit activity recorded as an electrical signal in the form of an EMG recording, gives an aggregate of the electrical contributions made by active motor units

[18]. The EMG can be usually measured using conductive metal electrodes. Two primarily different types of electrodes (and concepts) exist to record EMG signals. These two types are surface electrodes and indwelling or needle electrodes [16]. Needle electrodes are inserted into the muscle through the skin, while surface electrodes are placed on the skin directly over the muscle. Motor unit activity recorded using surface electrodes is termed surface electromyogram (sEMG) and possesses distinct advantages over motor unit activity recorded from indwelling electrodes. The advantages of sEMG recordings include safety, ease of operation and most importantly a non-invasive method of recording muscle activity [13].

The primary avenues for analyzing sEMG are studying the amplitude of the sEMG and spectral analysis of the sEMG [18]. The amplitude of sEMG is related to the recruitment and discharge rate of active motor units and early research efforts used sEMG activation as a reflection of the level of activation. However, sEMG amplitude is affected by a number of factors, prominent among which are the electrode location, thickness of skin and underlying tissues, distribution of motor unit conduction velocities, etc. These factors lead to a mismatch between the output of the CNS and the sEMG amplitude [19], [20]. Spectral analysis has been widely used to study changes in motor unit recruitment and muscle fatigue in the past. However, the generation and discharge of motor unit potentials is a transient phenomenon and as such, sEMG recordings are non-stationary in nature. The ability of spectral methods to analyze and glean useful information from non-stationary signals is at best limited. This has led to the increasing use of time-frequency methods of analysis to study sEMG signals. The efficacy of time-frequency domain methods to detect transient peaks in lower back muscles has been demonstrated in [21]. In

addition, the ability to distinguish movement and intensity from EMG data using time-frequency methods was shown in [22], [23], and the utility of the wavelet transform in effectively distinguishing motor unit action potentials was demonstrated in [24], [25].

1.2.3 Intent Recognition

Intent recognition is defined as the observation of actions, inference of goals and prediction of future actions, and is a fundamental capability required for human-machine interaction [1]. From the perspective of prostheses or assistive devices, intent recognition is defined as the recognition of a user's intent to perform a particular motion [26], and as these devices grow more technologically advanced and complex, intent recognition is increasingly becoming an integral part of the control scheme of prosthetic or assistive devices [5]. Intent recognition for prostheses and for most assistive devices predominantly utilizes surface electromyogram (sEMG) signals from the user's body [27]–[30]. Surface EMG signals are well suited for such intent recognition because the electrical potentials in muscles that correspond to muscular activity are generated 20 ms to 100 ms before activity occurs, and provide information regarding impending motion [16], [31]–[33]. With signals obtained from a user's body, implementing an intent recognition system essentially involves running a pattern classification scheme [34], [35], to classify and interpret patterns in the signals that correspond to intent and motion.

In addition to sEMG signals, the inclusion of other types of sensors used, the classification methods employed, and the signal processing techniques have an important bearing on any implementation of intent recognition. The next four subsections will take a closer look at intent recognition implementations in literature, specifically intent

recognition of the torso, intent recognition of assistive devices in general, and the classification methods and features used for intent recognition.

Intent Recognition of Back and Torso

Intent recognition of the upper body, back and torso primarily finds applicability in assistive devices for the torso [36]–[42]. Most of the available literature in this field generally touches upon the need for intent recognition or mentions implementation very briefly. However, detailed information on intent recognition of the upper body is found to be lacking in the existing literature. To the best of the author's knowledge, only two instances were found in the literature that provided any appreciable detail on this topic. The first of these two instances is an assistive device for the upper back called the Wearable Power Assist Suit (WPAS) [42], [43]. Photographs and a schematic of the device are shown in Fig. 1.3.

Figure 1.3: Photographs and schematic of WPAS [42].

The device shown in Fig. 3 is a five link device that spans the back of the torso and legs, with a single motor for actuation. To infer user intent, the device uses surface electromyogram (sEMG) sensors on the arms and legs, and position sensors on the torso

and limb joints. One of the related publications mentions an artificial neural network (ANN) was used for classification of sEMG data [43], however details or information about accuracy are not available.

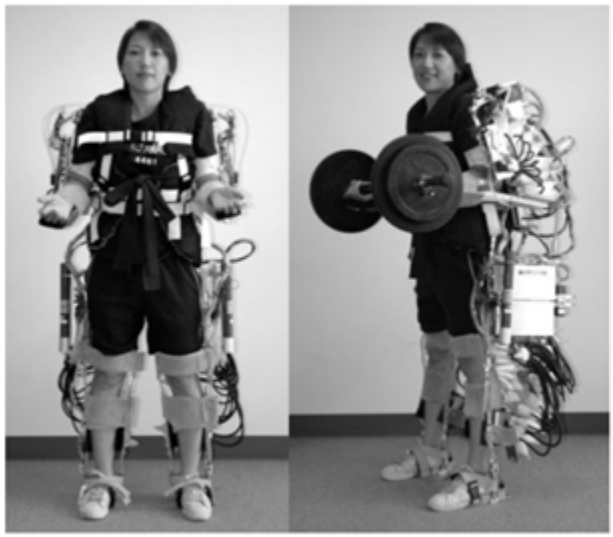

Figure 1.4: Photographs of Power Assist Suit in use [36].

The second device is called the Power Assist Suit, and is intended for providing assistance during lifting tasks encountered by nursing professionals [36], [44]. Two views of the device in use during a lifting task can be seen in Fig 1.4. The device is designed to provide assistance to the arms and torso and is pneumatically actuated. For inferring intent, the device uses muscles stiffness sensors and position sensors on the arms, legs and back. The muscle stiffness sensors are essentially contact pressure sensors mounted in contact with the muscles and function as a mechanical analogue of an electromyogram. It should however be noted that no information about the classification method used, or the accuracy of intent recognition is presented.

Intent recognition in general

In the wider world of intent recognition for other body segments such as arms, legs or prostheses, the available research literature is well developed and informative, and presents a wide variety of information about the sensors used and the classification methods employed [3], [27], [45]. An exemplary case of intent recognition for arm motion is shown in Fig. 1.5 [28].

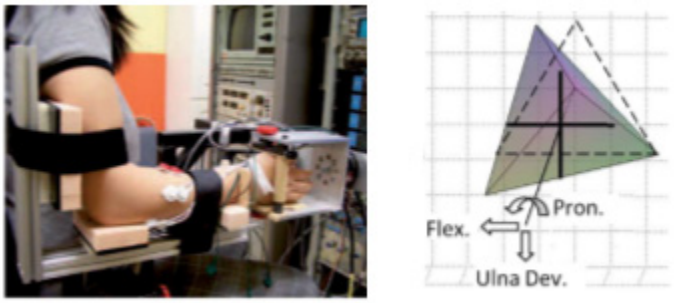

Figure 1.5: Intent recognition of arm movements using 4-channel sEMG [28].

Figure 1.5 shows a four-channel sEMG sensing setup on the forearm, to detect flexion/extension, radial deviation/ulnar deviation, and pronation/supination motions of the wrist. The paper presented a nonlinear classifier and demonstrated classification accuracy ranging from 75% to 90%. Another example intent recognition system for a transfemoral prosthesis is shown in Fig. 1.6 [4]. The sensing suite included six sEMG sensors, position sensors, and inertial sensors. The approach employed linear and Bayesian classifiers to classify flexion/extension, radial/ulnar deviation and pronation/supination motions of the wrist, and demonstrated classification accuracies up to 96%.

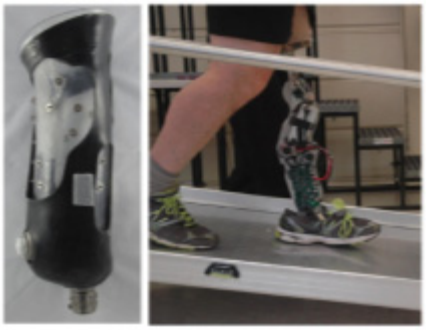

Figure 1.6: Intent recognition for transfemoral prosthesis using sEMG and inertial sensors [4].

Further survey of the current literature points to a preponderance of sEMG sensors used for detecting user intent [20], [28]–[30], [34], [46]–[50], followed by inertial sensors [2], [3], [5], [6], [51]. Some of the works have highlighted the limitations of solely using sEMG sensors and have presented approaches using a combination of sEMG and inertial sensors [4], [52], [53]. These publications have pointed out that using only sEMG delivers limited accuracy in classification, and have also shown that a combination of sEMG sensors with inertial sensors improves accuracy and reliability of classification. In all three of these publications, up to 12% improvement in classification accuracies was demonstrated as a result of combining sEMG and inertial sensors.

Classification Methods

In addition to sensors and sensing strategies, information about the methods used for classification of human activity and intent data is also available in the literature. The use of Bayesian decision theory and Bayesian parameter estimation methods was demonstrated with up to 96% classification accuracy in [45], [54], [55]. The use of linear methods such as linear discriminant analysis for classifying human physiological data to infer intent, was demonstrated in [5], [27], [47], [56], with classification accuracies

ranging from 82%-92%. Among nonlinear methods of classification, support vector machines (SVM) are currently very popular for classifying human activity and intent data, and instances with up to 98% classification accuracy can be seen in [35], [46], [57], [58]. In addition, multilayer neural networks, which have been the most popular nonlinear classifiers, have also been used with up to 98% classification accuracy, as evident in [28], [54], [57], [59], [60].

Of the classification approaches listed above, Bayesian methods require prior information about the probability distribution of the signals [37]. For an entirely new set of physiological data, this information is not available, and therefore Bayesian methods largely out of the scope of a data driven study such as the one described by this dissertation. Sample based linear methods such as perceptrons or linear discriminant analysis have been shown to be computationally efficient and mostly unsusceptible to overfitting [7], [8]. Moreover, projection based methods such as linear discriminant analysis have been shown to be able to classify multiple classes in a single-step, and are among the generally preferred linear classifiers [53]. On the other hand, nonlinear methods such as support vector machines and neural networks are notorious for being computationally complex and prone to overfitting [8].

Feature Extraction

Closely associated with the classification methods are the features used for extracting patterns from sEMG and other sensor data. Signals sampled from a physical system in the form of a time-series do not always reflect the entire information content of the measurement. Particularly, discriminating information that displays a large degree of separability between two measurements corresponding to two different states is not always

easily accessible from the raw data, and needs to be teased out from the mathematical and statistical properties of the signal data. Feature extraction is the most domain dependent aspect of a classification system, and it makes it possible to closely tailor a solution to a particular problem through the use of targeted, domain specific features [7], [61]. Traditionally, time-domain and frequency-domain were the most commonly used features [30], [62]. However, the advent and increasing accepting of time-frequency domain methods of analyses has led to wider adoption of time-frequency domain features extracted using the wavelet transform [25], [63], [64]. Of particular interest to this dissertation, is the selection of suitable wavelets for time-frequency domain feature extraction. Among the many families of wavelets the Daubechies family of wavelets has been found to be particular effective in analyzing sEMG recordings [35], [65], [64], [66], [67]. Multiple studies have pointed to the utility and effectiveness of multiple Daubechies wavelets from db-2 to db-8, and all the way up to db-20 [24], [25], [63], [68]. In addition, the use to feature statistics to reduce extracted features can also be seen in literature. Specifically, the use of mean absolute value, waveform length, zero crossings and sum of coefficients has been shown to be effective in reducing wavelet coefficients in [62], [69], [70].

1.3 Scope and Summary of Research

This work in this dissertation has three objectives that stem from the exploration of the space between linear and non-linear methods of classification. These objectives are to: (1) investigate and evaluate a set of non-linear features that can represent complex spatiotemporal patterns in time-series data; (2) identify and evaluate a suitable linear method of pattern classification, and establish a methodology to combine the features and method of classification; and (3) evaluate the performance of the combination of linear

classification and non-linear features in terms of classification accuracy, and benchmark the results against non-linear methods of classification.

In order to address the first objective, time-frequency domain features were investigated for representing spatiotemporal variations in physiological data. Specifically, the wavelet transform was employed to investigate and establish a targeted set of features for this purpose. To address the second objective, linear discriminant analysis (LDA) was selected as the method of classification. This is because it is computationally efficient and a data driven, sample based linear method of classification that makes minimal assumptions about the data. In addition a method of combining multiple features with LDA using a multi-classifier combination scheme is also presented. Furthermore, a method of fine tuning the classification performance through a weighted classifier combination is presented. To address the third objective, the combined classification, feature extraction and classifier combination methods were tested on a physiological data collected from three human subjects, and a classification accuracy of 97% was demonstrated. In order to benchmark these results, the performance of the multi-classifier LDA using nonlinear features was compared against the performance of nonlinear support vector machine classifiers, and the classification performance was shown to be comparable to that of non-linear methods of classification.

1.4 Organization

This dissertation is organized into five chapters. Chapter 1 presents the introduction, motivation, review of literature and scope of this project. To address the objectives listed in the scope and evaluate the performance of the proposed method of classification, a physiological dataset was assembled. Chapter 2 outlines the experimental

design and collection of the dataset used. Chapter 3 presents the extraction of nonlinear features from the physiological data, the theoretical background and methodology involved in implementation of a multi-classifier LDA, and the combination of multiple features. Before these methods were established, a preliminary study of a two-class LDA was conducted on a subset of the data. The results of this two-class study are detailed in Appendix B. Chapter 4 evaluates the performance of the combination of linear classification and non-linear features in terms of classification accuracy, and benchmarks the results against non-linear methods of classification. Finally, Chapter 5 presents the conclusions and future directions.

CHAPTER 2

INTENT RECOGNITION DATASET

To enable the development of the proposed methods of nonlinear feature extraction, linear classification and classifier combination, and to evaluate the performance of the proposed methods, a physiological dataset was assembled, by collecting data from three human subjects. In order to closely represent the motivating problem and to tightly focus on one set of motions, this dataset consisted of data corresponding to only flexion and extension motions of the torso in the sagittal plane.

It would be necessary for the physiological data input to the activity and intent recognition system, to encompass information that can help predict impending activity to recognize intent, and information about the kinematic state to recognize activity. Knowing that sEMG voltage appears in muscles about 20 ms – 100 ms before activity occurs [16], it becomes possible to access information that can help predict impending motion by reading sEMG activity from muscles. Moreover, state information and information needed for activity recognition can be acquired by employing inertial sensors (accelerometers and gyroscopes) on the body.

In order to analyze flexion and extension motions in the sagittal plane, the focus of this study is limited to muscle groups that are directly causal to this motion. These muscle groups correspond to flexor and extensor muscles of the back and abdomen. Moreover, muscle activity is recorded in a non-invasive manner at the surface of the skin and the readings are logged as surface electromyogram (sEMG) signals. Furthermore, inertial signals are recorded from multiple sensor locations on the back.

2.1 Experimental Design

An experimental study was designed to collect the required sEMG and inertial signals. The study involved human participants and was approved by the University of Massachusetts – Institutional Review Board (IRB). A listing of the participants' physical characteristics is shown in Table 2.1.

Table 2.1: Physical Characteristics of Study Participants.

Participant	Age	Height	Weight
Participant 1	24 years	1.71 m	61 kg
Participant 2	24 years	1.67 m	60 kg
Participant 3	25 years	1.75 m	63 kg

The sEMG signals were recorded from the flexor and extensor muscles of the back and abdomen using a commercial sEMG measurement system (Delsys™). The measurement system uses 12 electrodes (10 mm spacing; Ag-AgCl) sampled at 1.2 kHz to record muscle activity. Eight electrodes were placed on the back and four were placed on the abdomen.

Electrode mounting sites corresponded to multiple locations on the erector spinae (L1, L3, T9 levels) and latissimus dorsi on the back, and the rectus abdominis and external obliques on the abdomen. The electrode mounting sites were decided based on input from literature related to EMG measurement [13], [71], [72], and are listed in Table 2.2. A photograph of the sEMG sites, with the electrodes attached to a test participant can be seen in Fig. 2.1. A 60s plot of the 12 sEMG channels is shown in Figs. 2.2, 2.3 and 2.4.

Table 2.2: sEMG Electrode Mounting Locations.

Sensor Number	Muscle Location
1, 2	Erector Spinae, L3 (Left, Right)
3, 4	Erector Spinae, L1 (Left, Right)
5, 6	Erector Spinae, T9 (Left, Right)
7, 8	Latissimus Dorsi (Left, Right)
9, 10	Rectus Abdominis (Right, Left)
11, 12	External Obliques (Right, Left)

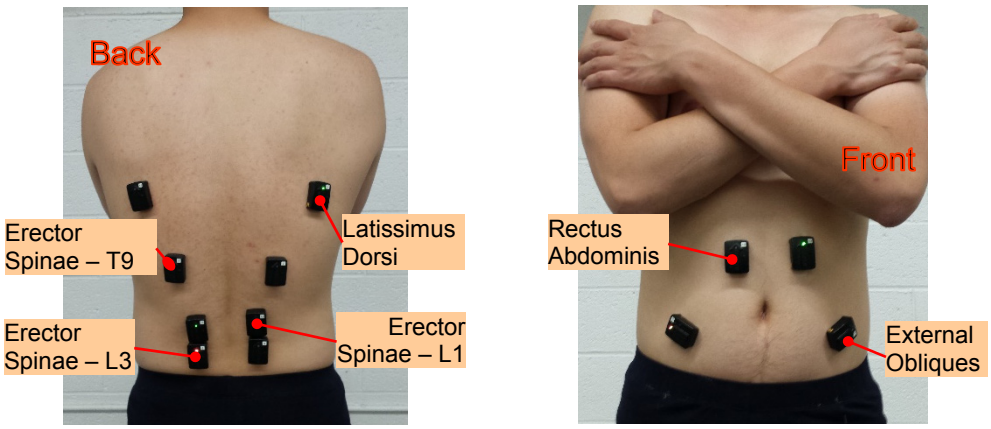

Figure 2.1: Electrode mounting sites.

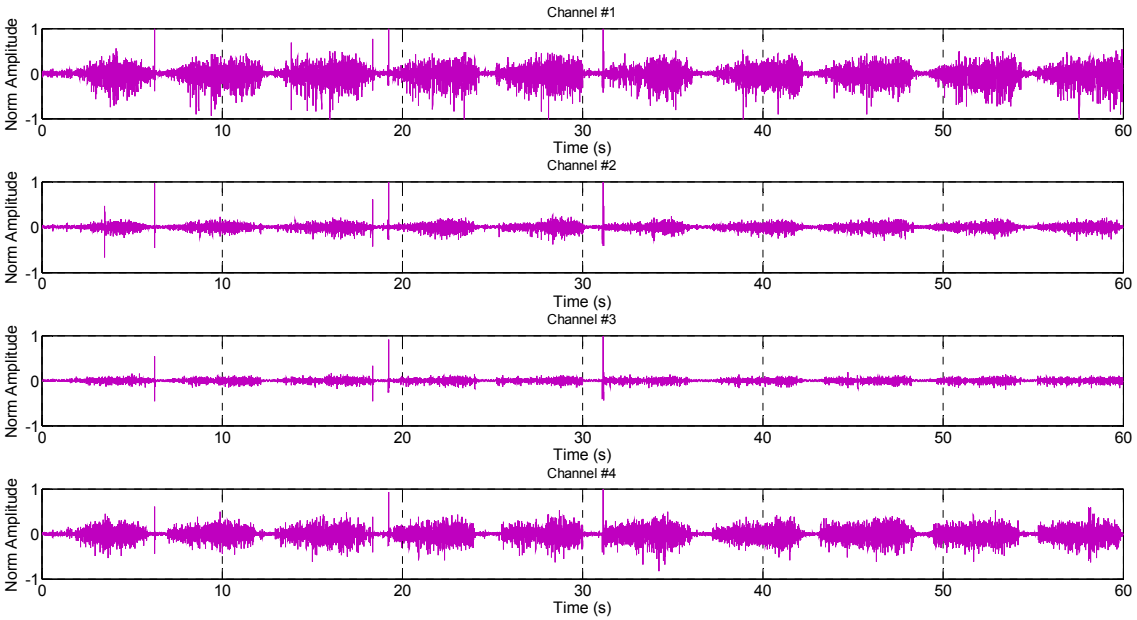

Figure 2.2: Channels 1-4 of sEMG data; 60s recording of flexion and extension motions.

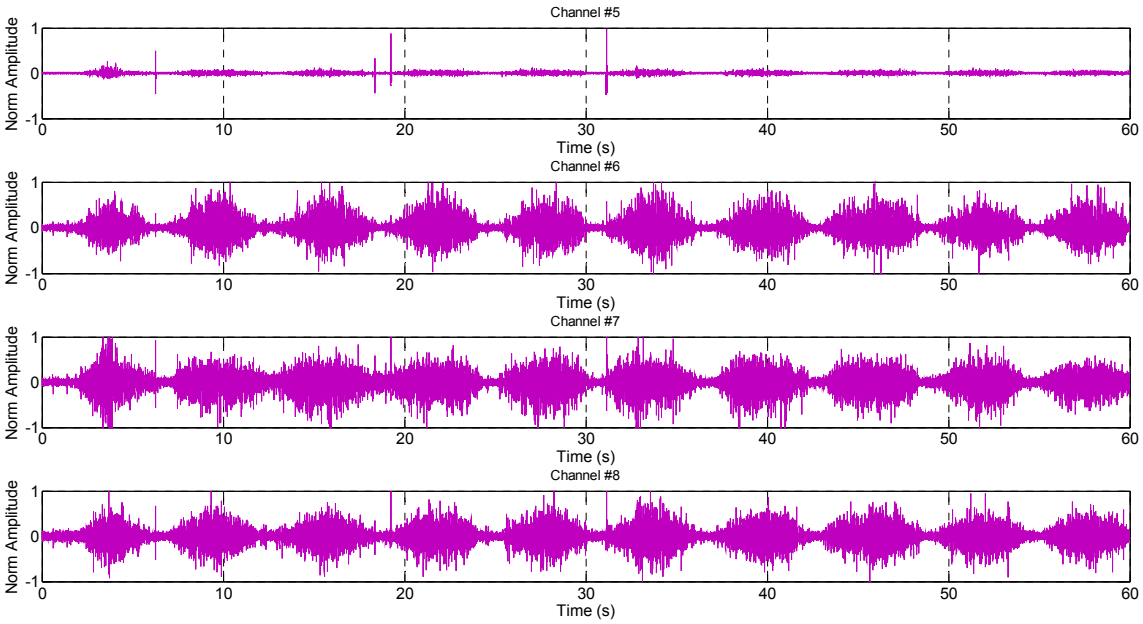

Figure 2.3: Channels 5-8 of sEMG data; 60s recording of flexion and extension motions.

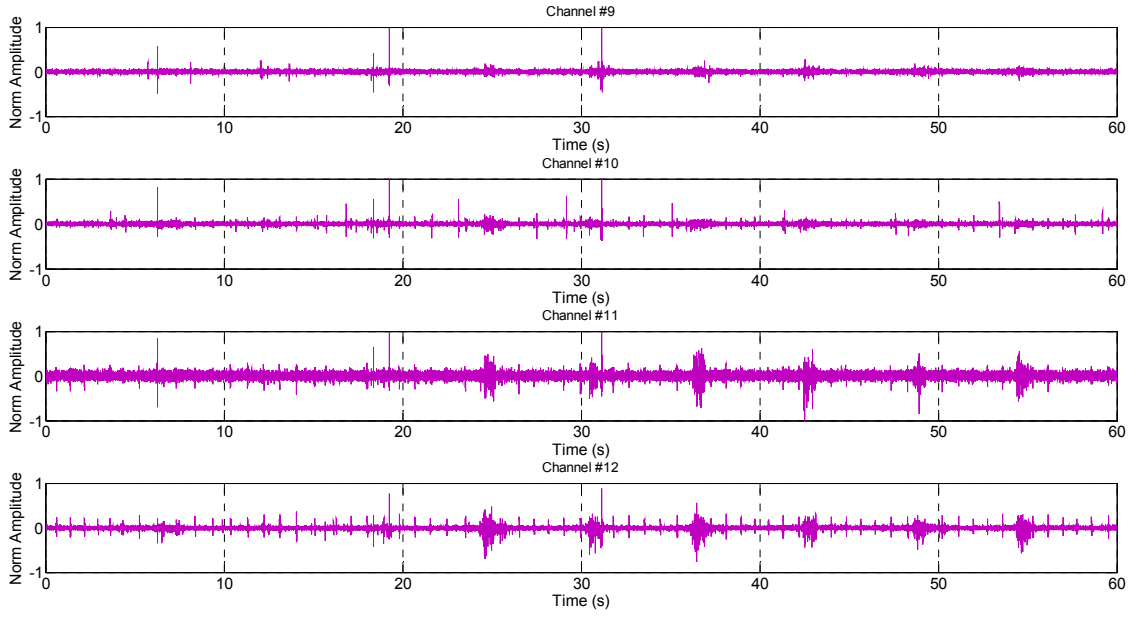

Figure 2.4: Channels 9-12 of sEMG data; 60s recording of flexion and extension motions.

Kinematics were obtained by using a high-speed motion capture system (Qualisys™ – Oqus), which was synchronized with the sEMG measurement in order to ensure a common time-stamp on all the recordings. The motion capture system sampled motion at 240 Hz and used groups of reflective markers placed at anatomical locations on the participant's body, to define points of interest. Principal marker placement was at the sacrum, and at the L1, T7, T4 and C7 vertebrae. These vertebral locations were used to divide the back into four distinct segments that were assumed to be rigid body segments for the purpose of studying motion [16]. The lumbar segment was defined from the sacrum to the L1 vertebra, the region between the L1 and T7 vertebrae was designated the lower thoracic segment, the region between the T7 and T4 vertebrae was designated the mid-thoracic segment, and the T4 and C7 vertebrae demarcated the upper thoracic segment.

In this dissertation, data from inertial measurements have been emulated using motion capture data. Rigid planar clusters of markers, as shown in Fig. 2.5, were placed on each of the segments to accurately define and track the motion of each segment. These clusters were used to emulate inertial sensors: the first derivative of the angular deflection of a cluster emulates the 'rate' output of a gyroscope, and the linear acceleration of the centroid of each cluster is analogous to the output of an inertial accelerometer.

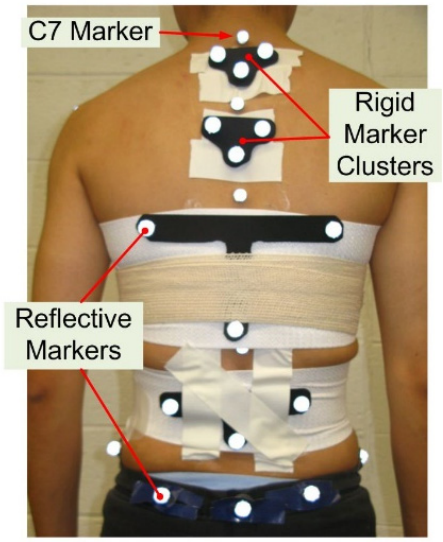

Figure 2.5: Optical Marker Placement for Emulating Inertial Sensors.

2.2 Experimental Protocol

The sEMG electrodes and reflective markers were affixed to the body of a research participant, who performed specific movements of the torso. The movements studied were flexion and extension in the sagittal plane. Starting from a normal standing position, the participant was asked to bend forward such that the torso made a roughly 90° angle with the coronal plane. This constituted the flexion movement, and the return from the bent position to the standing position constituted the extension movement. These movements were performed for different speeds to complete one flexion-extension movement, over a number of tests. A metronome was used to set the speed for each trial. A listing of the experimental protocol is shown in Table 2.3. This protocol is a subset of a larger study to collect data for a wider variety of motions. Details of the larger study can be found in Appendix A.

Table 2.3: Experimental Protocol.

	Activity	Speed	Duration
1)	Stand in neutral position	-	30 s
2)	Flexion/Extension – Bend forward and stand back up	60 bpm	120 s
3)	Flexion/Extension – Bend forward and stand back up	120 bpm	120 s
4)	Stand in neutral position	-	30 s
5)	Flexion/Extension – Bend forward and stand back up	184 bpm	120 s
6)	Flexion/Extension – Bend forward and stand back up	208 bpm	120 s
7)	Flex forward 30° and hold position	-	60 s
8)	Flex forward 60° and hold position	-	60 s
9)	Hyper-extend 5° and hold position	-	60 s
10)	Hyper-extend 15° and hold position	-	30 s
11)	Stand in neutral	-	30 s

2.3 Pre-Processing

The sEMG signals recorded from the system corresponded to a bandwidth of 20 Hz – 450 Hz. These preprocessing for these signals included subtracting any offset from the signals and normalizing the signals in magnitude, by dividing the signal amplitude by the largest magnitude observed. No additional filtering operations were performed. The inertial signals were bandpass filtered between 5 Hz – 30 Hz, detrended to eliminate offset, and inclinations were calculated from the inertial measurements.

2.4 Data Segmentation

To enable classifier generation (training) and testing the pre-processed signals were partitioned into activities of interest. As mentioned earlier, the activities of interest for this study are flexion and extension in the sagittal plane. These activities correspond to the

states or classes that will be used to define and generate classifiers. In addition to these two states, another state referred to as ‘dwell’, has been defined to represent inactivity.

While collecting data, a set of motion capture cameras were continuously monitoring the motions of the subjects. From this motion capture feed, it was possible to accurately localize the commencement and conclusion of each activity. Accordingly, segments of the pre-processed signals corresponding to the commencement and conclusion of each activity and the interim period of inactivity (flexion, extension and dwell), were isolated into separate chunks of data that were subsequently used for classifier generation and testing.

The resulting dataset consisted of 12 sEMG signals and 4 inertial signals, from each of the three subjects. For classifier generation, segmented and labelled data corresponding to one of three states – flexion, extension and inactivity was made available. The classifiers so generated were tested on segmented data, as well as on a simulated real-time stream of data that represented continuous real life activity.

CHAPTER 3

MULTI-CLASSIFIER FUSION APPROACH

This chapter presents a multi-sensor, multi-classifier intent recognition approach that uses Linear Discriminant Analysis (LDA) for pattern classification. Critical to the performance of any linear classification method like LDA, are the features that are used to obtain separability in the data to enable classification. The use of targeted non-linear features with a linear classification method, to deliver improved classification accuracy is also discussed. Specifically, the identification and extraction of time-frequency domain features using wavelet transform methods, that can help deliver improved classification performance is discussed.

Building upon traditional LDA, a multi-classifier method of classification is presented, which utilizes multiple classifiers combined together using a majority voting classifier fusion scheme. In addition a weighted multi-classifier combination method for combining outputs of multiple classifiers to deliver improved classification accuracy is also presented.

3.1 Theoretical Background

3.1.1 Pattern Classification for Intent Recognition

As mentioned earlier, the problem of recognizing intent from sensor data is essentially one of classifying patterns occurring in sensor data. In this scenario, pattern classification primarily pertains to assigning pre-defined labels to objects [61] in a data-set. The objects themselves can be defined by a set of measurements, attributes or features,

and the objective here is to construct a discriminant or prediction rule for assigning labels to objects [73]. Such a discriminant rule is generally a projection method that looks to maximize the separability between different objects in a data set.

Among the various discriminant analysis methods, sample-based linear methods are appealing because of their simplicity of implementation. Some additional advantages of following sample-based, linear methods of discriminant analysis are that they can be purely data driven, do not require any prior information about the data, and allow minimum assumptions to be made about the nature of the data.

Linear Discriminant Analysis

Fisher's Linear Discriminant Analysis is one such linear method of generating discriminants that seeks to project data in a manner such that separability between different objects in a dataset is maximized. In addition, while seeking maximum separability it also seeks a projection that minimizes the variance of a particular feature within the dataset.

This discriminant is constructed by seeking a function w, that projects data x, consisting of a number of classes n, onto (n-1) lines y, such that maximum separation is achieved between the classes [74], as shown in (1).

$$y = w^T x \tag{1}$$

The measure used to separate the classes is the mean of the classes, μ_i, shown in (2), where N_i is the number of samples in each class.

$$\mu_i = \frac{1}{N} \sum_{x \in \omega_i} x \tag{2}$$

This separation is achieved by maximizing a function w, which represents the difference between the means of the classes normalized by the variance in the classes. This

maximization can be solved as an eigenvalue problem dependent on the scatter within the classes S_W, and the scatter between the classes S_B. This is an eigenvalue problem that essentially reduces to the expression in (3).

$$S_W^{-1} S_B w = \lambda w \tag{3}$$

The variance of each class can be quantified by the scatter of the class, defined in (4) below.

$$S_i = \sum_{x \in \omega_i} (x - \mu_i)(x - \mu_i)^T \tag{4}$$

The summation of the scatter of all classes gives the 'within-class scatter' S_W, expressed in (5) below.

$$S_W = \sum_i S_i \tag{5}$$

The variance between the classes is quantified by the 'between-class scatter' S_B. For data that contains m classes, it is expressed as in (6).

$$S_B = \sum_{i=1}^{m} N_i (\mu_i - \mu)(\mu_i - \mu)^T \tag{6}$$

The eigenvectors obtained from (3) yield the projections w, which are the classifiers used to separate the data. This projection is called Fisher's linear discriminant and gives the directions for projecting the data such that maximum separation is achieved between classes.

Multiple Classifiers

The accuracy of classification obtained from LDA can be improved by using multiple classifiers. The advantages of using multiple classifiers are threefold [61]. From the statistical point of view, combining multiple classifiers helps to average the outputs of

multiple classifiers and avoid having to select a single best classifier that might not be adequate by itself. From the computational viewpoint, combining multiple classifiers can help avoid possible local optima. Thirdly, from the representational point of view, there is a possibility that the solution space of a particular problem might not encapsulate the optimal classifier. In such a case, multiple classifiers can possibly approximate the solution more accurately. Multiple classifiers can be combined using two major strategies. These are classifier fusion and classifier selection. Classifier fusion utilizes approaches such as averaging or majority voting to obtain classification accuracy that is better than that can be obtained from the individual classifiers. Classifier selection involves choosing the best classifier out of a set of multiple classifiers. When it comes to biomechanical signals, it has been shown that fusion based approaches deliver better results with a combined accuracy far better than any single classifier [75], [76]. Therefore the adoption of a fusion based approach, specifically majority voting based fusion is proposed to improve upon the classification performance of traditional LDA.

3.1.2 Feature Extraction

Signals sampled from a physical system in the form of a time-series do not always reflect the entire information content of the measurement. Particularly, discriminating information that displays a large degree of separability between two measurements corresponding to two different states is not always easily accessible from the raw data, and needs to be teased out from the mathematical and statistical properties of the signal data.

Time Domain and Frequency Domain Features

Traditionally, time-domain and frequency-domain features were commonly employed for extracting discriminating information from sensor generated signals, and a previous study by the author of this dissertation has also investigated these features [53]. These features are commonly used as a starting point in similar studies, and are listed here to serve as a point of comparison against subsequent studies. The features extracted were the mean absolute value, the variance, the signal length, the spectral energy and the three most prominent frequency components, and are explained below [30], [62].

1) Mean Absolute Value

The Mean Absolute Value (*MAV*), is the average of the absolute value of a signal x_i, in a window of n samples and is expressed in (7). It provides a quantifiable measure of muscle contraction levels and is therefore a principal feature in processing sEMG data.

$$MAV = \frac{1}{n}\sum_{i=1}^{n}|x_i| \tag{7}$$

2) Variance

The variance *var*, provides a measure of the signal power. It is expressed in (8) below.

$$var = \frac{1}{n-1}\sum_{i=1}^{n}\left(x_i - \bar{x}\right)^2 \tag{8}$$

3) Waveform Length

The waveform length *WL*, shown in (9) is representative of the complexity in the signal, and is defined as the cumulative length of the signal over a time segment. It possesses information about amplitude and frequency of the signal.

$$WL = \sum_{i=1}^{n} \left| x_i - x_{i-1} \right| \tag{9}$$

4) Spectral Energy

The spectral energy E_S, helps identify the periodicity in the signal, and is calculated from Fourier transform components X_k, that are calculated from the signal x_n, as shown in (10) and (11).

$$E_S = \frac{1}{N} \sum_{n=0}^{N-1} \left| X_k \right|^2 \tag{10}$$

$$X_k = \sum_{n=0}^{N-1} x_n e^{-ik 2\pi n / N} \tag{11}$$

5) Frequency Components

The frequency components a_k, are calculated from Fourier series coefficients as shown in (12). The first three coefficients in order of decreasing absolute magnitude are selected as features.

$$a_k = \frac{1}{N} \sum_{n=0}^{N-1} x_n e^{-ik 2\pi n / N} \tag{12}$$

Time-Frequency Domain Features

Knowing that human motion and sEMG data are non-stationary in nature, the major focus of this study is on time-frequency domain features. Implementation of time-frequency domain feature extraction is achieved by using the wavelet transform. Previous research on the applicability and use of wavelets in analyzing sEMG data and for feature extraction has generated a substantial amount of literature, as has been listed in the review of literature. This abundant research record is useful in selecting operating parameters such as wavelet bases, the method of wavelet decomposition, and other nuances of feature

extraction. The applicability of wavelet transform feature extraction to classification problems involving sEMG and other related signals is evident in a number of research efforts [21], [25], [29], [34], [49], [50]. On a narrower level, a number of studies have highlighted the utility of the Daubechies family of wavelets in representing sEMG waveform [22], [49], [63]. Another interesting aspect of wavelet transform based extraction methods is the use of statistical moments calculated from wavelet coefficients, which were introduced in [65]. These research studies help inform our choice of wavelet bases and feature statistics, for use in the current study.

3.2 Methods

The proposed multi-sensor, multi-classifier approach towards intent recognition is made up of a number of different methods. This section discusses the methods employed in this study. An overview of the methods used in this approach is shown in Fig. 3.1.

The workflow starts with the collection of physiological data from human subjects performing flexion and extension motions in the sagittal plane, which was presented in the previous chapter. The next step discusses extraction of features, where wavelet bases are employed to elicit time-varying properties from signals, and feature statistics are run over the coefficients to reduce the dimensionality of feature vectors. The next stage deals with selecting the best subset of features, from the total set of features obtained from the feature extraction stage. This is followed by classification, where three different approaches are discussed.

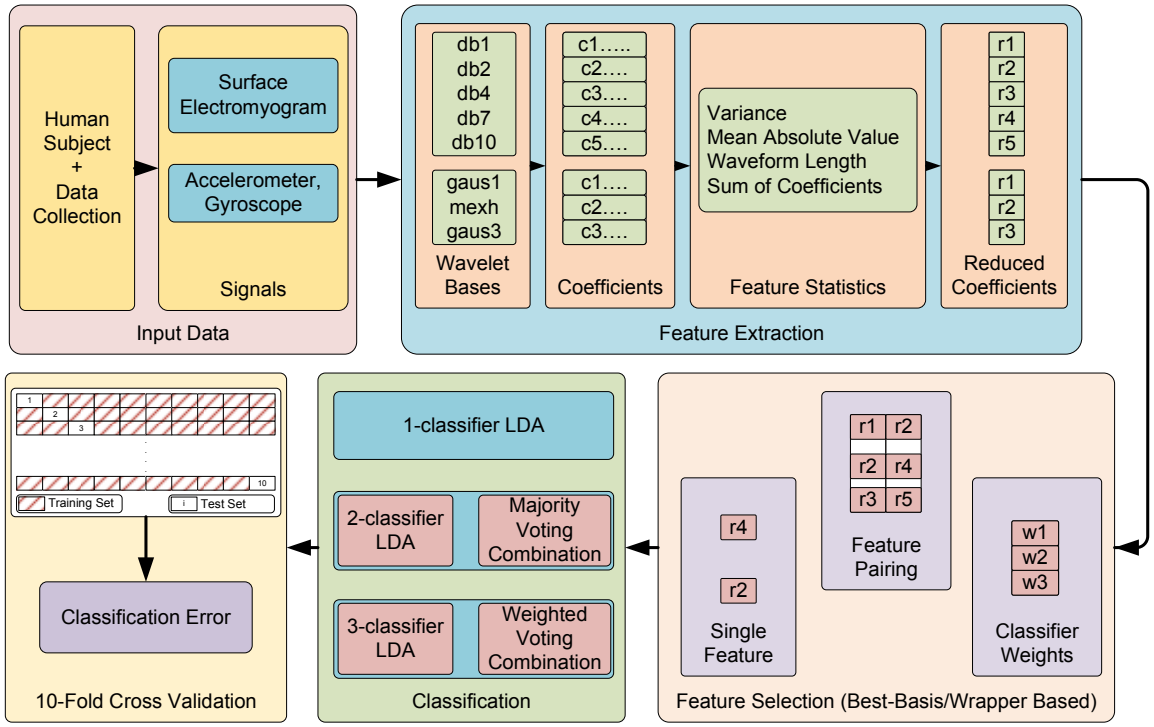

Figure 3.1: Flow diagram illustrating methods employed in this analysis.

3.2.1 Feature Extraction

As mentioned earlier, the wavelet transform has been employed to extract targeted time-frequency domain features from the input data. Specifically, a coarse-grained form of the continuous wavelet transform (CWT) have been employed to extract features from the data. The mathematical expression for a general CWT is shown in (13) below.

$$C = \frac{1}{\sqrt{a}} \int_{-\infty}^{\infty} x(t) \psi^* \left(\frac{t-b}{a} \right) dt \tag{13}$$

In the equation above, ψ^* is the mother wavelet, b is the translation parameter, a is the scaling parameter, and C is the set of coefficients generated from the wavelet decomposition. To this equation, coarse graining is applied such that the usual fine resolution of the frequency scales is avoided by using exponential scales with a base equal to 2 in the scaling parameter a, as shown in (14).

$$a = 2^k; k = [1, 2, ...7] \tag{14}$$

Due to the coarse graining of the frequency scales, finer frequency resolution is traded off for faster computation time. This is a viable trade-off because we are interested in discriminating features in a broad region of interest that spans 37.5 Hz – 150 Hz for the sEMG data and 1 Hz – 10 Hz for the inertial data. The erector spinae muscles are known to have EMG activity in a broad range of frequencies from 70 Hz to 120 Hz [77]. These choice of two adjacent wavelet space frequency bands, from 37.5 Hz – 75 Hz and 75 Hz – 150 Hz encompasses the frequency range of the muscles and helps to obtain a targeted feature space for the muscles.

During implementation, sliding windows of width 512 samples (426 ms) were used for the wavelet decomposition described in (13). In other words, a 512-point wavelet decomposition was carried out at every stage. After every decomposition, the sliding window was shifted by 24 samples (20 ms) to capture data for the next stage.

The selection of wavelet bases ψ^*, in (13) is primarily informed by available literature, but at the same time knowing that wavelet representation is an exercise in template matching, wavelets that match the shapes of the waveforms shown in figures 9-11 are desirable. Accordingly, for the sEMG signals, five bases from the Daubechies family of wavelets were used as basis functions, and for the inertial signals the Gaussian and its derivative wavelets were used as basis functions. Studies have shown that erector spinae activity occurs within a 75 Hz – 90 Hz range [77], and accordingly the 75 Hz – 150 Hz and its adjacent 37.5 Hz – 75 Hz frequency sub-bands were selected for extracting coefficients. Moreover, the coefficient arrays obtained from (13) were further consolidated into a single

'feature statistic'. A listing of the wavelet bases and associated feature statistics is shown in Table 3.1.

Table 3.1: List of Mother Wavelets and corresponding Feature Statistics.

	Feature Number	Wavelet Name (Symbol)	Feature Statistic	Frequency Sub-band
sEMG Features	1	Daubechies-1 (db1)	Sum of absolute coefficients	75 Hz – 150 Hz
	2	Daubechies-1 (db1)	Waveform length	75 Hz – 150 Hz
	3	Daubechies-2 (db2)	Variance	75 Hz – 150 Hz
	4	Daubechies-4 (db4)	Sum of absolute coefficients	37.5 Hz – 75 Hz
	5	Daubechies-4 (db4)	Sum of absolute coefficients	75 Hz – 150 Hz
	6	Daubechies-4 (db4)	Mean absolute value	37.5 Hz – 75 Hz
	7	Daubechies-7 (db7)	Sum of absolute coefficients	37.5 Hz – 75 Hz
	8	Daubechies-7 (db7)	Mean absolute value	37.5 Hz – 75 Hz
	9	Daubechies-10 (db10)	Waveform length	37.5 Hz – 75 Hz
Inertial Features	10	Gaussian (gaus1)	Sum of coefficients	0 Hz – 9.375 Hz
	11	Mexican Hat (mexh)	Sum of coefficients	0 Hz – 9.375 Hz
	12	Second derivative of Gaussian (gaus3)	Sum of coefficients	0 Hz – 9.375 Hz
	13	Fourth derivative of Gaussian (gaus5)	Sum of coefficients	0 Hz – 9.375 Hz

3.2.2 Classification

The features obtained from the feature extraction stage were used in the generation and testing of classifiers. Initially, a single classifier was generated through a 3-class LDA. The three classes were defined as a) Flexion in the sagittal plane, b) Extension in the sagittal plane, c) Dwell, or inactivity. Features were extracted every 20 ms using a 512 ms overlapping time window, and fed to an LDA routine. For a 3-class LDA, eqn. (3) generates two Eigen vectors, and the Eigen vector corresponding to the larger Eigen value is chosen as the LDA projection, *w*. The classification performance of the classifier generated from this analysis was evaluated using an iterated ten-fold cross validation method. After the

single-classifier LDA was tested, a multi-class classifier as detailed below was implemented and evaluated.

Multi-Classifier Strategy

In order to improve upon the performance afforded by a single classifier, a multi-classifier combination strategy has been adopted. This approach is based on the idea that combining the opinions of an ensemble of individual classifiers can possibly result in a better opinion [61], [78]. The basic premise of the strategy employed in this paper, can be encapsulated in the flowchart shown in Fig. 3.2. As seen in the figure, multiple features are extracted from the sensor data, and individual classifiers are generated from each feature. The class labels generated by all the classifiers are subsequently combined to generate a final classification result that is informed by the contributions of all the classifiers involved. Specifically, each of the 9 sEMG features were paired up individually with every one of the rest, to generate 36 possible pairs of features. After studying these pairs or 2-classifier combinations, every one of the pairs was then combined with a single inertial feature, to generate 36 3-classifier combinations.

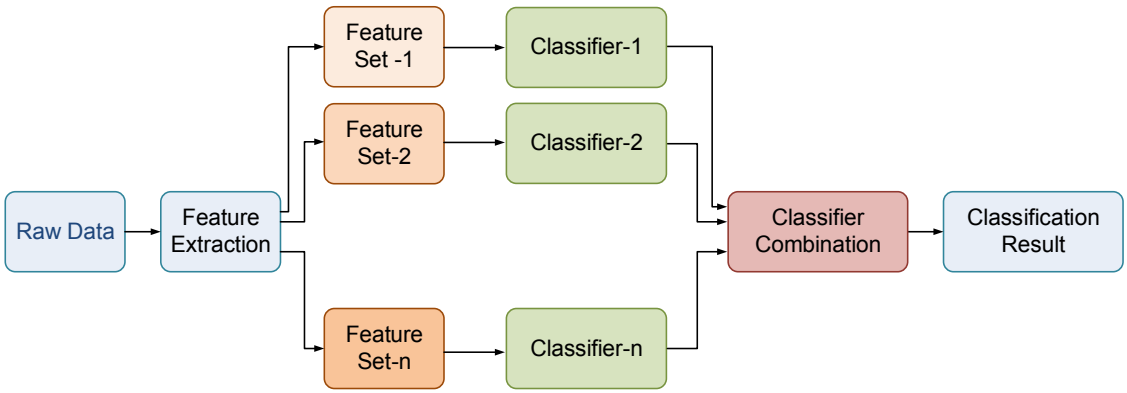

Figure 3.2: Flowchart depicting multi-classifier strategy.

Classifier Combination

To combine the multiple classifiers mentioned in the immediate previous section, two kinds of combination methodologies were investigated. These are defined in the following equations.

Simple majority voting fusion

This is a simple plurality voting scheme, where a simple summation of the class labels is used to implement classifier combination.

$$k_i = \max_{n=1}^{N} \sum_{i=1}^{m} k_{i,n} \tag{15}$$

In the equation above, k is the class label, m is the number of classes and N is the number of classifiers.

Weighted majority voting fusion

If classifiers in a group are not of identical accuracy, then it is reasonable to bias/weight the classifiers in a manner such that more accurate classifiers can have more of a say in the final result. This can be implemented according to (16) below.

$$k_i = \max_{n=1}^{N} \sum_{i=1}^{m} b_i d_{i,n} \tag{16}$$

In (4), d is the initial (individual) class label, k is the final (resulting) class label, m is the number of classes, N is the number of classifiers, and b is a numerical weight assigned to the classifier.

In practice, a 3-dimensional quantity has been designed to accompany every classifier output. The classifier output itself is a numerical label that identifies the class,

and the 3-dimensional quantity is the weight assigned to that particular classifier. This weight w, can be expressed as shown in (17) below.

$$w = \begin{bmatrix} i & j & k \end{bmatrix} \tag{17}$$

In (17), i, j, k, are numerical values ($0 \le i, j, k \le 1$) that represent the confidence of the classifier in predicting a class. When outputs from multiple classifiers are obtained, they are combined via summation of the columns of the matrix shown in (18).

$$\sum w = \begin{bmatrix} i_1 & j_1 & k_1 \\ i_2 & j_2 & k_2 \\ i_3 & j_3 & k_3 \end{bmatrix} \tag{18}$$

After summation of the columns, the three values are compared and the maximum of the three resulting values is then designated as the combined classifier output. The individual weights are designed such that the maximum possible sum of a column is 1.

Model Selection

The preceding three sections have discussed features, feature groupings and weights for combining features/classifiers. The selection of features, feature sets and their respective weights is treated as a model selection problem, guided by a variant of a Local Discriminant Bases algorithm based on the Best-Basis Paradigm [79], [80]. The Best-Basis Paradigm is a three step process that involves 1) establishing a collection of features or bases 2) sorting the features by a property relevant to the problem 3) selecting the best surviving feature.

For a classification algorithm such as LDA, the defining property is the separation between different classes in a recorded data stream. Generally, a measure known as the cross entropy or relative entropy, which is calculated from the probability distribution of

each class, is used as a defining property. In the absence of any probability information, the next best measure of separation is the classification performance of the feature on a subset of data. Accordingly, a wrapper based selection method [81], where a collection of features was evaluated for classification performance on a subset of the data, was adopted. The available data was segmented into a training set, two validation sets and a test set, as shown in Fig. 3.3. The classifiers generated from the training set were tested on the first validation (Val^n-1) set to select the best feature set, and subsequently tested on the second validation set (Val^n-2) to select the best weighted feature set. The performance of the resulting classifier was finally evaluated on the final test set.

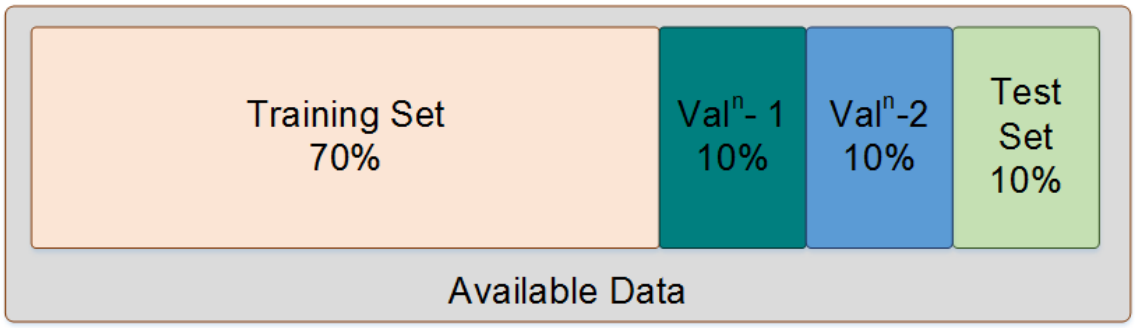

Figure 3.3: Data segmentation for feature selection.

3.2.3 Classifier Performance

The performance of the features and classifiers discussed above needs to be evaluated in order to ensure that they can classify new, but similar data. This performance is quantified in terms of the classification error and classification accuracy. The classification error is defined as the ratio of the number of data points misclassified to the total number of data points in the test set. The error, when multiplied by 100 gives the 'error rate', which is expressed as a percentage. The classification accuracy is obtained by subtracting the percent error rate from 100%, and is also expressed as a percentage. While

collecting data, a set of motion capture cameras were continuously monitoring the motions of the subjects. From this motion capture feed, ground truths corresponding to flexion, extension and dwell were established for all the collected data. During evaluation, classification results were compared against the ground truth to ascertain whether a particular result was a correct classification or a misclassification.

The performance of the classifiers in correctly classifying every one of the classes involved is noted separately. In other words, three different accuracy values (corresponding to each class) are reported for a 3-class classifier. Furthermore, validation of classifier performance is achieved by splitting a set of labelled data into two mutually exclusive subsets. Classifiers obtained via training on of one of the subsets called the 'training set', are evaluated on the second subset called the 'test set'. In order to evaluate the feasibility and usefulness of a sEMG augmented intent recognition system, this work employs a more rigorous ten-fold cross validation method.

In ten-fold cross validation, the available data is segmented into 10 subsets and ten iterations of simple validation as defined above, are carried out. During each iteration, one of the 10 subsets is used as the 'test set' and the other 9 subsets are combined together to form the 'training set'. A single classifier is generated from the 'training set' and evaluated for classification accuracy on the 'test set'. A schematic illustration of this procedure is shown in Fig. 3.4.

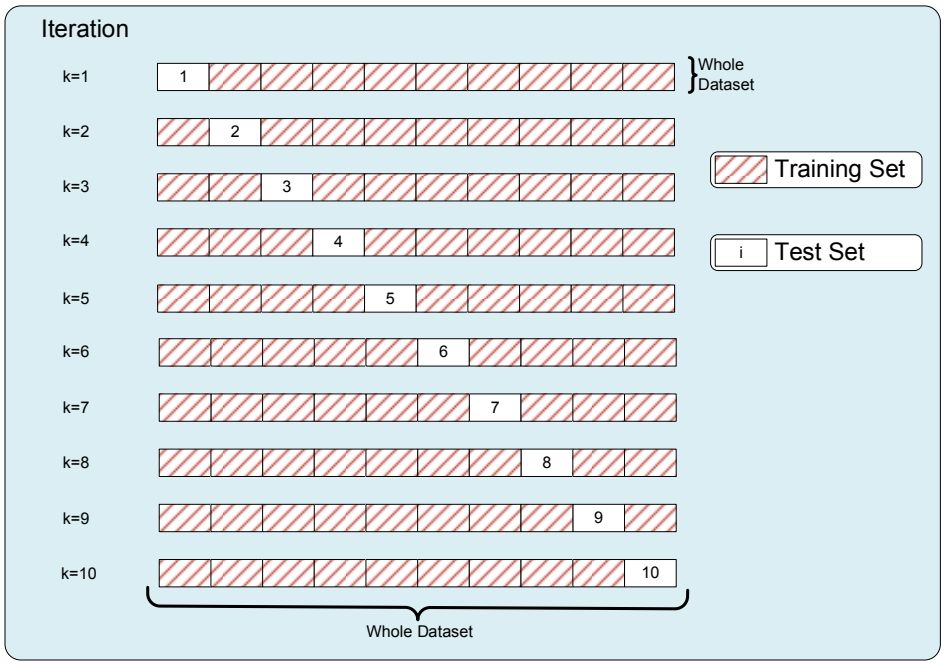

Figure 3.4: Schematic diagram of 10-fold cross validation.

CHAPTER 4

EVALUATION OF MULTI-CLASSIFIER FUSION APPROACH

The intent recognition approach presented in the prior chapter uses non-linear time-frequency domain features with a linear classifier. In order to quantify its performance and benchmark against other classifiers, this section presents results obtained from evaluation of the presented approach. As a first step, traditional time-domain and frequency-domain features were employed with the multi-classifier approach, to serve as a point of comparison. Subsequently, targeted time-frequency domain features were employed and the results are discussed in this chapter.

In addition, an empirical comparison between linear discriminant analysis (LDA), multi-classifier LDA and support vector machines (SVM) classifiers, using time-domain, frequency-domain, and time-frequency domain features is also presented. Comparison is performed on a single physiological dataset (explained in Chapter 2) and across a single metric – classification accuracy. The choice of a particular algorithm to address a problem presents a possible trade-off in terms of computational complexity, accuracy, susceptibility to noise and overfitting, etc. Moreover creative use of features with these algorithms can significantly alter the behavior of any of these algorithms. As the 'No Free Lunch' Theorem suggests there is no single universally supreme learning algorithm [82]. So, the evaluation and comparison of a multitude of algorithms, parameters and features is a non-trivial problem.

4.1 Time-Domain and Frequency Domain Features

To serve as a comparison point, classification results using traditional time-domain and frequency-domain features are first presented. Two different schemes of classification were employed. The first scheme was a simple classification scheme that generated a single all-encompassing classifier for all the seven time-domain and frequency-domain features extracted from the data. The second scheme was a multi-classifier classification scheme using the same time-domain and frequency-domain features. According to this scheme, individual classifiers were generated for each of the seven features, and the classification results of the seven classifiers were subsequently combined using a majority voting scheme.

A comparison of the classification error rates of classifiers generated from inertial data and from an augmented dataset (inertial and sEMG data combined in a single dataset), according to the simple classification scheme is shown in Fig. 4.1. The classification error rates of the all the three constituent classes are represented graphically and listed in Table 4.1.

Table 4.1: Classification Error Rates for Single Classifier.

Dataset	**Classification Error Rate**		
	Flexion (Class-1)	Extension (Class-2)	Dwell (Class-3)
sEMG	24.9%	72.3%	45.4%
Inertial	49.7%	51.3%	7.2%
sEMG + Inertial	34.7%	35.6%	6.1%

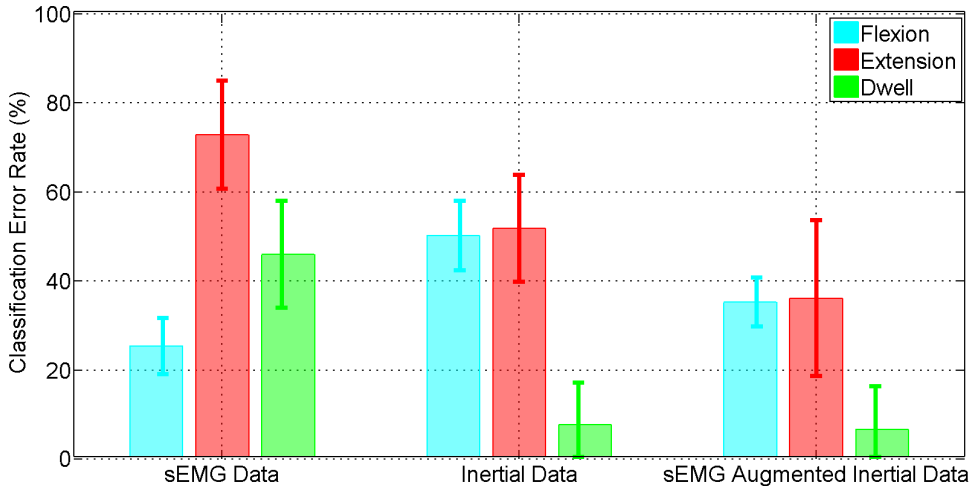

Figure 4.1: Classification performance - single classifier; Time-domain and frequency-domain.

From the graph, it can be observed that augmentation of inertial data with sEMG data improves classification performance by up to 30%. However, it should be noted that this classification performance can be considered modest at best and is largely unsuitable for interfacing with a human operator. The classification performance of the enhanced classification scheme, which generates multiple classifiers from a dataset, is shown graphically in Fig. 4.2 and tabulated in Table 4.2.

Table 4.2: Classification Error Rates for Multiple Classifiers.

Dataset	**Classification Error Rate**		
	Flexion (Class-1)	Extension (Class-2)	Dwell (Class-3)
sEMG	25.3%	76.3%	40.8%
Inertial	34.9%	35.2%	5.5%
sEMG + Inertial	8.3%	9.1%	2.3%

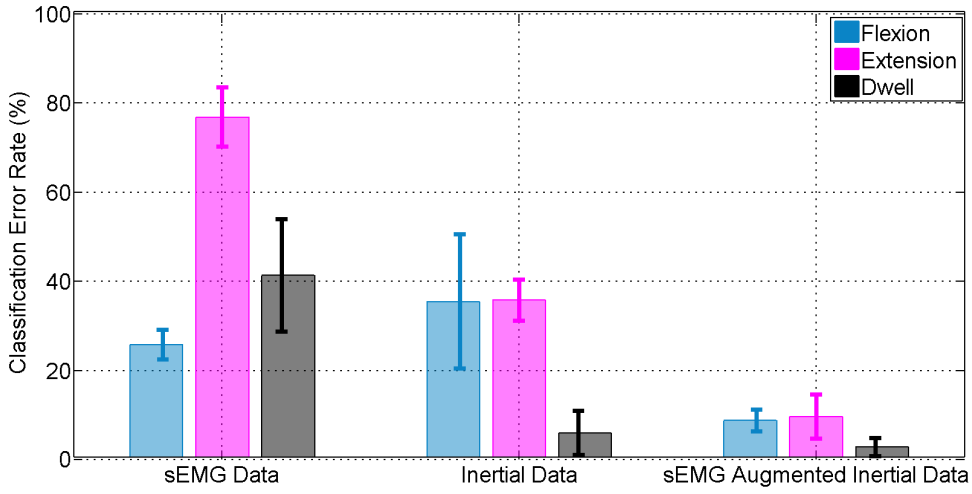

Figure 4.2: Classification performance - multiple classifiers; time-domain and frequency-domain.

It can be inferred from Fig. 4.2 that augmentation of inertial data with sEMG data substantially improves classification performance. In addition, comparing Fig. 4.1 with Fig. 4.2, we see that the majority voting based enhanced classification scheme delivers better classification performance than the simple, single classifier based scheme.

The most significant improvement in classification can be seen in the case of flexion and extension. The primary actuators for flexion and extension are the rectus abdominis muscles and the erector spinae respectively. These muscles are more prominent than most other muscles from which sEMG data was recorded and it can be surmised that sEMG data recorded from these muscles was the primary contributor in improving classification and reducing the classification error.

4.2 Time-Frequency Domain Features

The evaluation of the targeted non-linear time-frequency domain features with a linear classifier is presented in this section.

4.2.1 One-Classifier LDA, sEMG data

A three-class, single classifier LDA was run on each of the thirteen features listed in Table 4, extracted individually from the data collected from the three subjects. Features 1-9 were extracted from twelve sEMG channels and features 10-13 were extracted from four inertial channels. The classification performance of all these features for the three subjects is shown graphically in Figures 4.3-4.8. Figures 4.3 and 4.4 depict the performance of sEMG and inertial features respectively for Subject #1, Figures 4.5 and 4.6 depict the classification performance of sEMG and inertial features respectively for subject #2, and Figures 4.7 and 4.8 shown the performance of sEMG and inertial features respectively for subject #3.

From Fig. 4.3, it can be observed that the best available classification accuracy for flexion is 65% for subject #1. A similar inference can be made from Figures 4.5 and 4.7, where it can be observed that the best available classification accuracies during flexion for subject #2 and subject #3 are 65% and 70 % respectively. For extension, the best possible classification accuracy was observed to be 90% for subjects #1 and #2, and 85% for subject #3. For dwell, the sEMG features managed barely 50% for subject #1, up to 70% for subject #2 and a best case of 94% for subject #3.

On the other hand, looking at Figures 4.4, 4.6 and 4.8, classification accuracies of 60%-90% for flexion, 95% for extension and up to 98% for dwell, were obtained using features extracted from inertial data. However, it needs to be pointed out that these classification accuracies were mutually exclusive, and it can be observed that no single feature displays equal classification accuracy for all three classes.

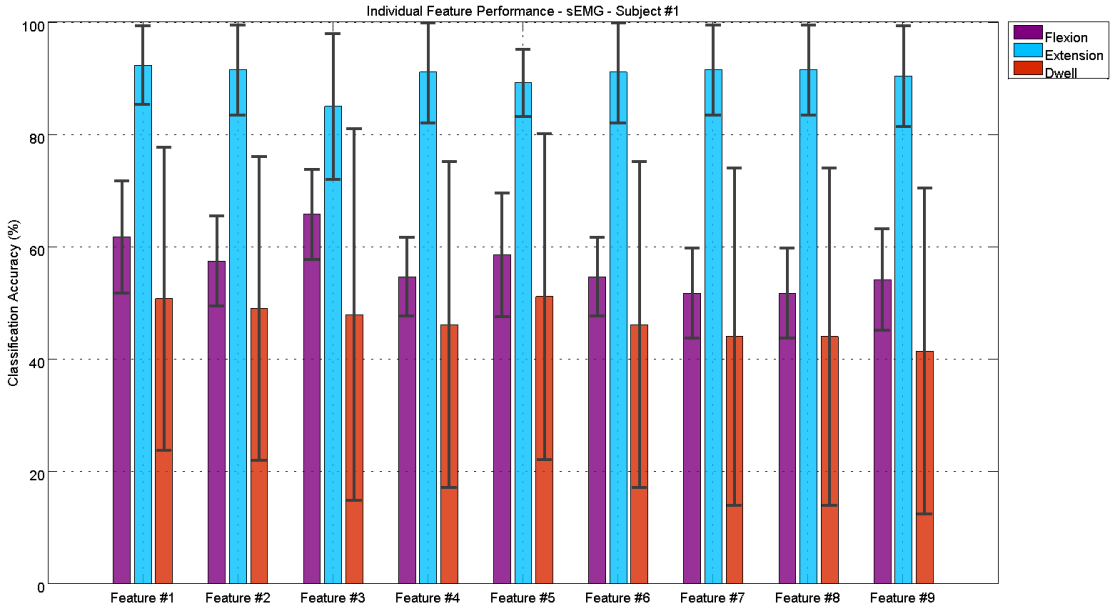

Figure 4.3: Classification performance of individual sEMG features with 1-Classifier LDA; Subject #1.

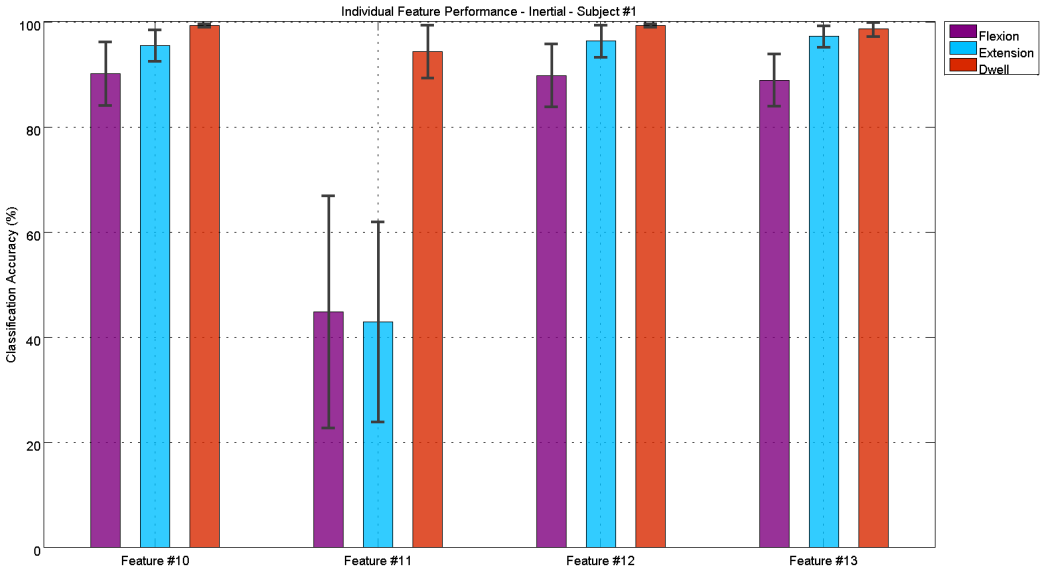

Figure 4.4: Classification performance of individual inertial features with 1-Classifier LDA; Subject #1.

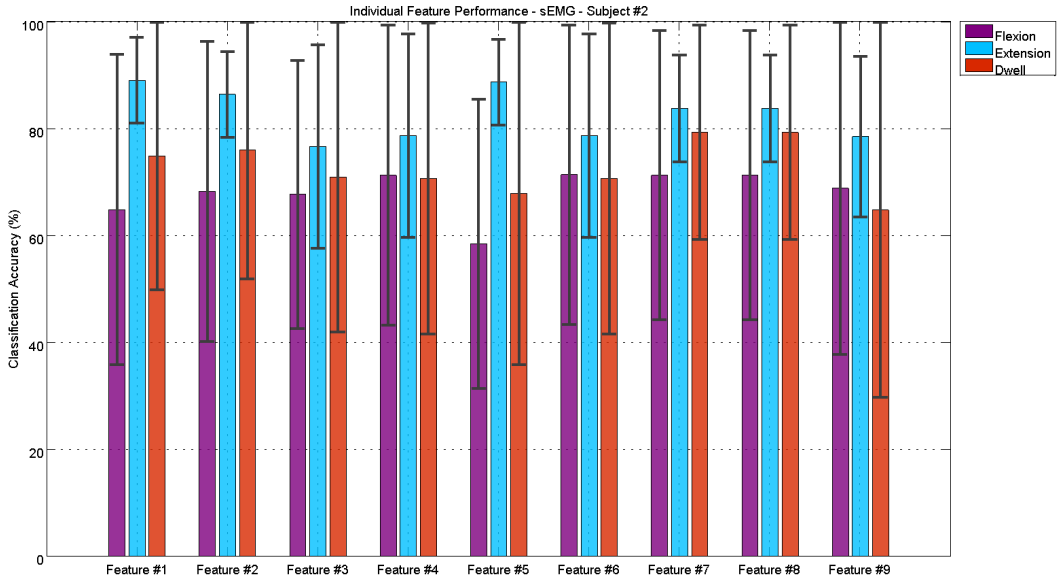

Figure 4.5: Classification performance of individual sEMG features with 1-Classifier LDA; Subject #2.

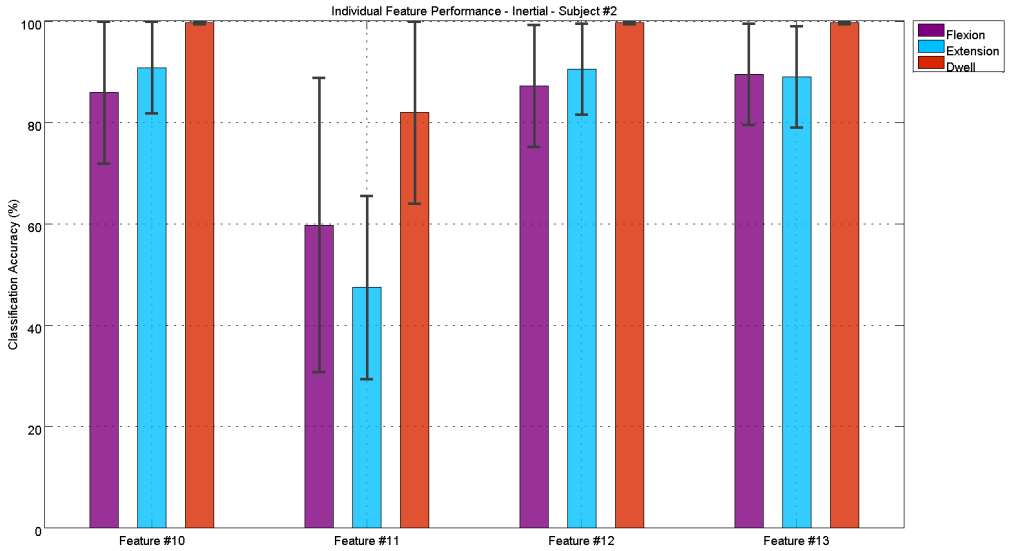

Figure 4.6: Classification performance of individual inertial features with 1-Classifier LDA; Subject #2.

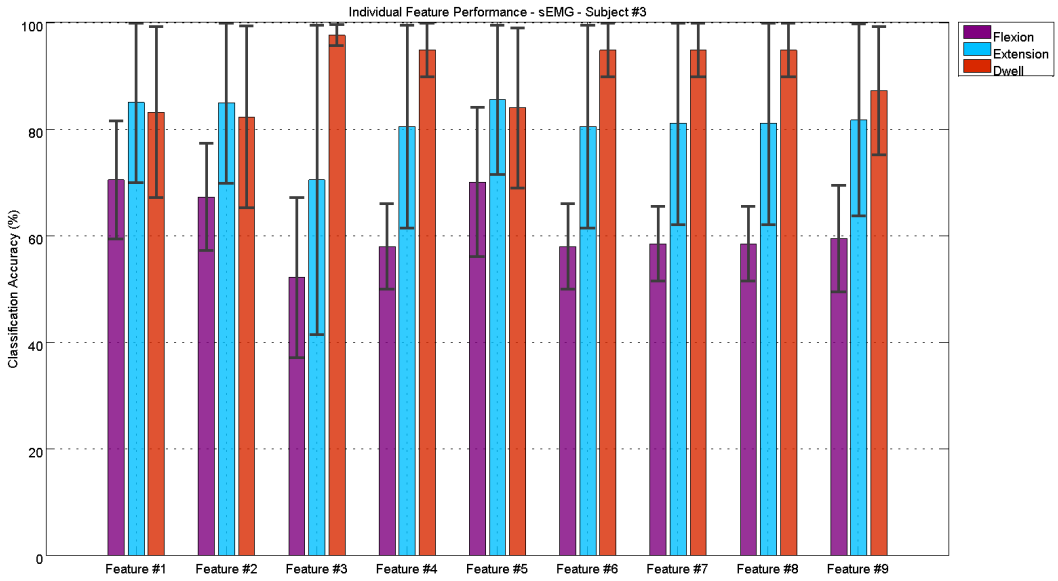

Figure 4.7: Classification performance of individual sEMG features with 1-Classifier LDA; Subject #3.

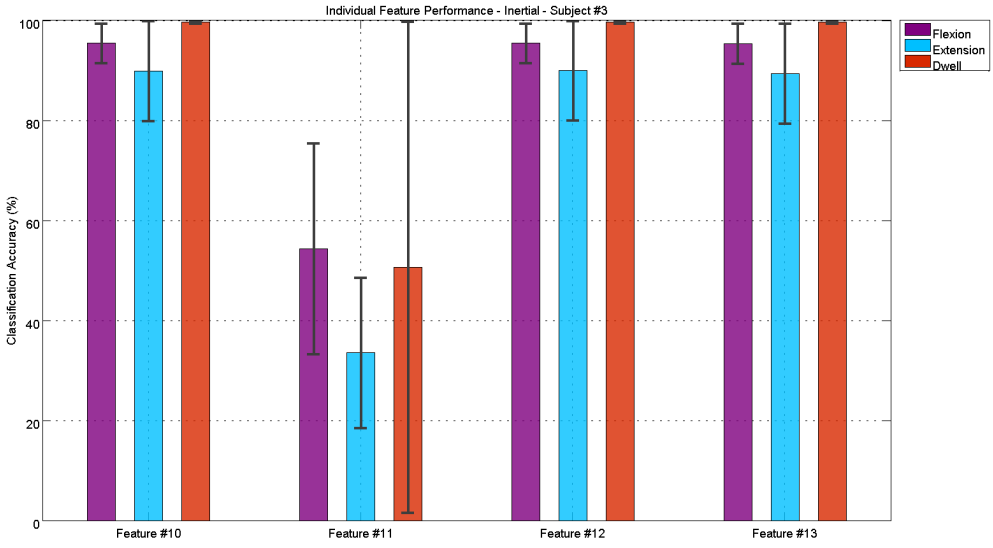

Figure 4.8: Classification performance of individual inertial features with 1-Classifier LDA; Subject #3.

4.2.2 Two-Classifier Majority voting combination

Subsequent to the 1-classifier LDA, the nine sEMG features were paired together to study the benefits of combining classifiers. All possible combinations of the 9 features, taken 2 at a time were considered. The number of possible feature pairs is given by the binomial coefficient (${}^{n}C_{r}$) and comes to 36 in this case (${}^{9}C_{2}$). Figure 4.9 illustrates the classification performance of all 36 feature pairs for subject #1. Similarly, Figures 4.10 and 4.11 show the classification performance of the 36 feature pairs for subjects #2 and #3 respectively.

Comparing Fig. 4.9 with Fig. 4.3, we see a very dramatic improvement in the classification accuracy for flexion from 65% to 97%, as evidenced from feature pairs #2, #9, and #16 - #21. Considerable improvement in the classification accuracy of extension from 90% to 96% can be observed in feature pairs #27 - #29, among others. On the other hand, no improvement in classification accuracy for dwell is observed.

Extending the same comparison to Fig. 4.10 and Fig. 4.5, an improvement in the classification accuracy for flexion from 65% to 80% can be observed in feature pairs #7 - #9. The classification accuracy for extension can also be observed to have improved slightly from 90% to 95%, which can be seen in feature pairs #3-#7 and #11-#14. However, the classification accuracy for dwell does not appear to shown any significant improvement. Similarly, comparing Fig. 4.11 and Fig. 4.7, the classification accuracy for flexion can be observed to have increased from 70% to 80%, as seen in feature pairs #11, #22, #27 and #28. For extension, looking at feature pairs #4, #5 and #27, the classification accuracy can be observed to have increased from 85% to 92%. Moreover, the classification

accuracy for dwell also appears to show marginal improvement from 94% to 96%, as can be observed from feature pairs #13 - #15 and #19 - #21.

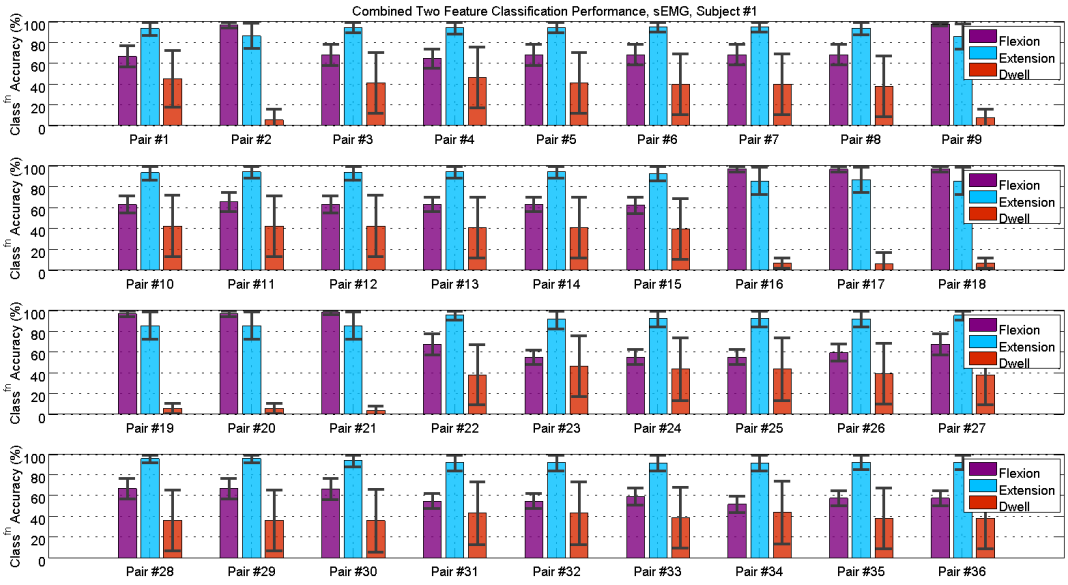

Figure 4.9: Classification performance of sEMG feature pairs with 2-Classifier LDA; Subject #1.

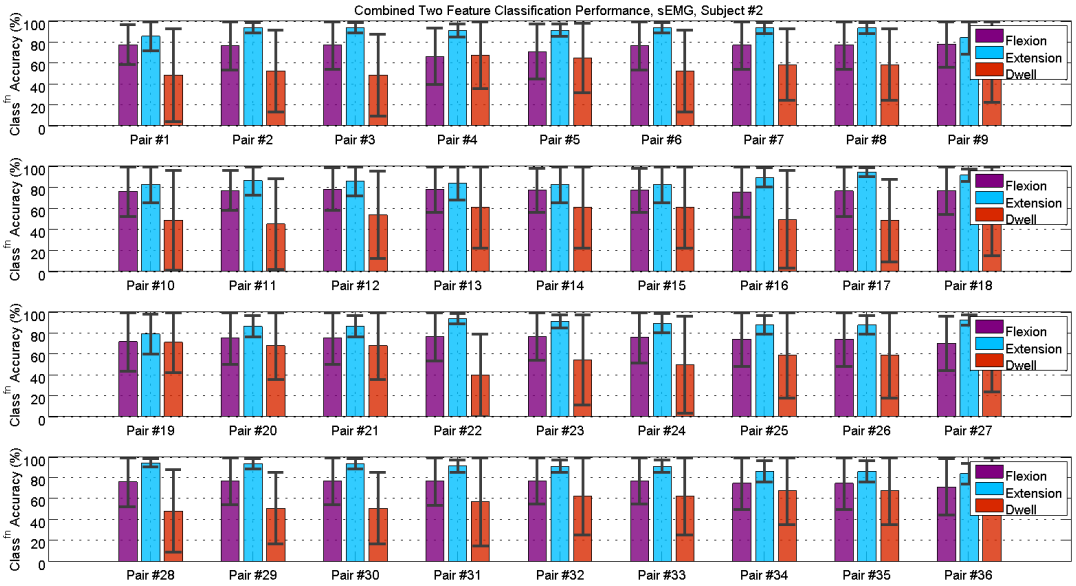

Figure 4.10: Classification performance of sEMG feature pairs with 2-Classifier LDA; Subject #2.

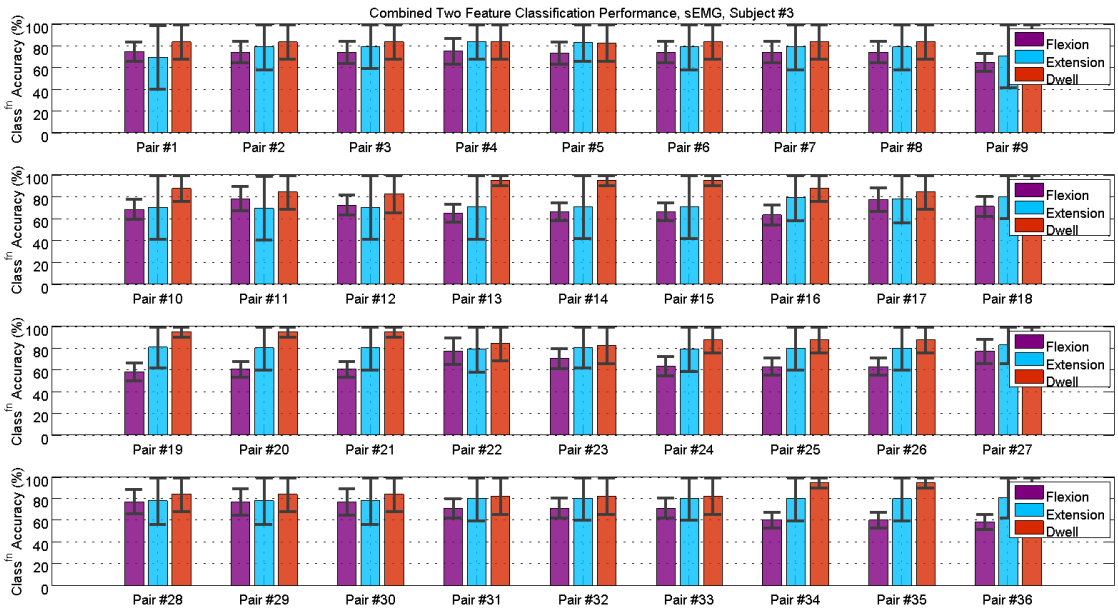

Figure 4.11: Classification performance of sEMG feature pairs with 2-Classifier LDA; Subject #3.

From Figures 4.9-4.11 and from the preceding discussion, it can be inferred that combining two classifiers provides substantial improvement in classification performance. This is especially true in the case of flexion and extension. However, this improvement in classification accuracy is not all round in the sense that it does not extend to all three classes, for all the subjects. Moreover, no single feature pair exists that delivers similar classification performance for all the three classes.

Another inference from this discussion is that sEMG features are very well suited for classifying flexion and extension, but not dwell. However, from Figures 4.4, 4.6, 4.8 we see that features extracted from the inertial signals deliver up to 98% classification accuracy for dwell. So the next logical step is to combine the sEMG feature pairs with a single inertial feature, in an attempt to combine the classification performance of the two sets of signals.

4.2.3 Three-classifier Majority voting combination

A 3-classifier approach, with one inertial feature and two sEMG features was tried next. Each of the 36 pairs from the previous test were combined with one inertial feature (gaus1, feature #10), to generate 36 sets comprising of 3 features. A 3-classifer LDA with simple majority voting combination was carried out to determine the classification performance of these feature sets. Figure 4.12 illustrates the classification performance of all 36 feature sets for subject #1. Similarly, Figures 4.13 and 4.14 show the classification performance of the 36 feature sets for subjects #2 and #3 respectively.

From Figures 4.12-4.14, it can be observed that some of the feature sets display comparable classification performance for two classes. This can especially be seen in feature sets #1, #9, #10, #11 for subject #1 in Fig. 4.12, where the classification accuracies for flexion and extension can be observed to be around 95%. However, in the rest of the cases no noticeable improvement in the classification accuracy can be observed. In fact, it can also be observed that the classification accuracy for flexion has dropped in certain cases, when compared to Fig. 4.9.

Table 4.3: Features and Weights for Weighted Classifier Combination.

Subject	Feature Index	Feature Name	Weight Vector
Subject #1	#1	db1 – Sum of absolute coefficients	[0.3, 0.5, 0]
	#2	db1 – Waveform length	[0.3, 0.5, 0]
	#9	gaus1 – Sum of coefficients	[0, 0, 1]
Subject #2	#2	db1 – Waveform length	[0.3, 0.45, 0]
	#5	db4 – Sum of absolute coefficients	[0.3, 0.45, 0]
	#10	gaus1 – Sum of coefficients	[0, 0, 1]
Subject #3	#2	db1 – Sum of absolute coefficients	[0.3, 0.5, 0]
	#5	db4 – Sum of absolute coefficients	[0.25, 0.5, 0]
	#10	gaus1 – Sum of coefficients	[0, 0, 1]

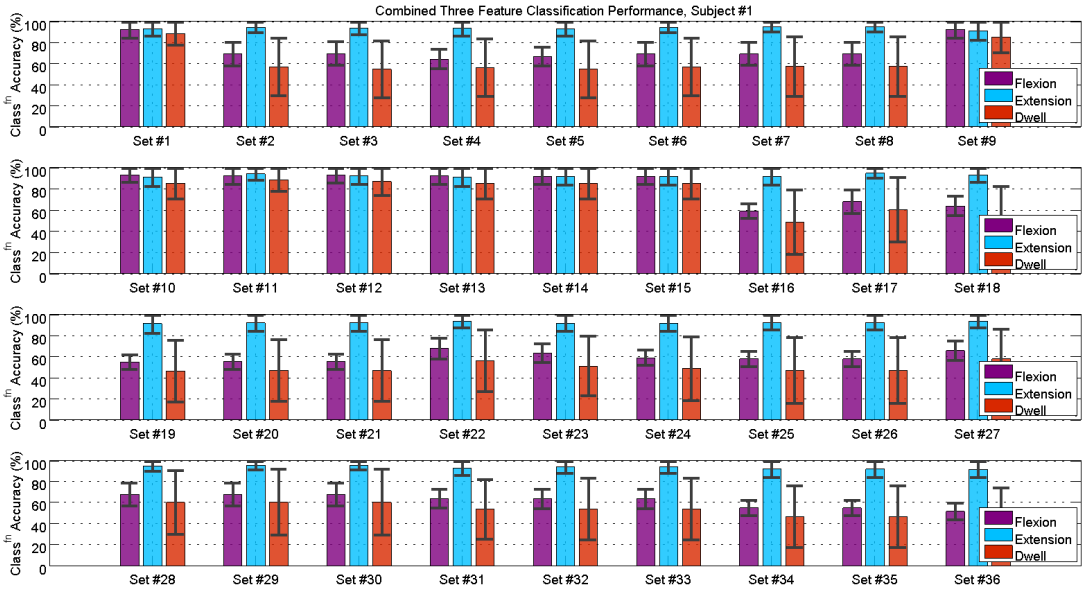

Figure 4.12: Classification performance of 3-Classifier LDA – 2 sEMG + 1 Inertial features; Subject #1.

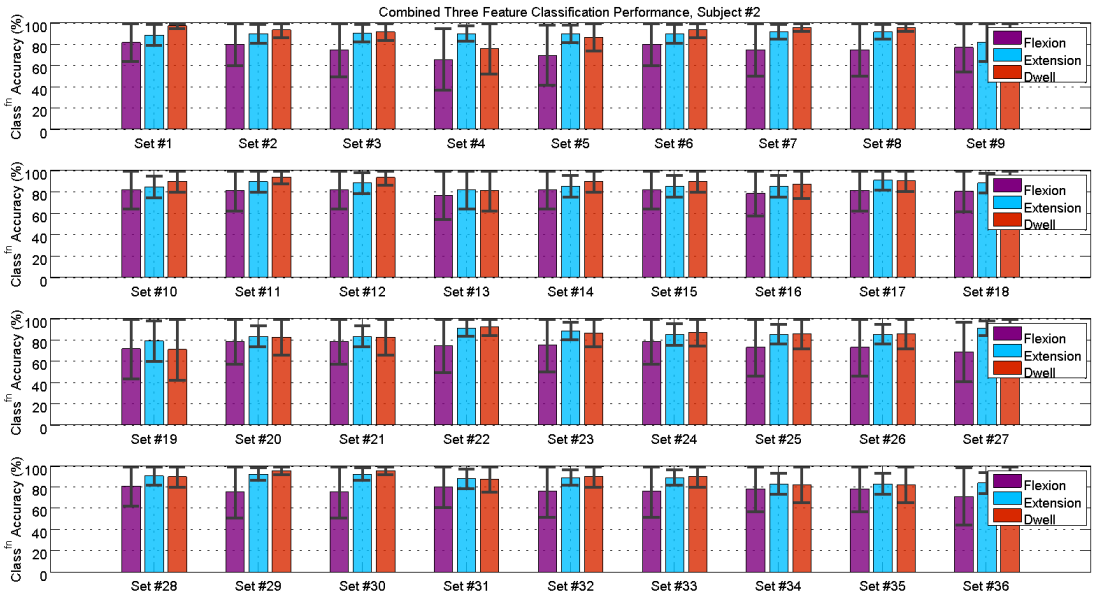

Figure 4.13: Classification performance of 3-Classifier LDA – 2 sEMG + 1 Inertial features; Subject #2.

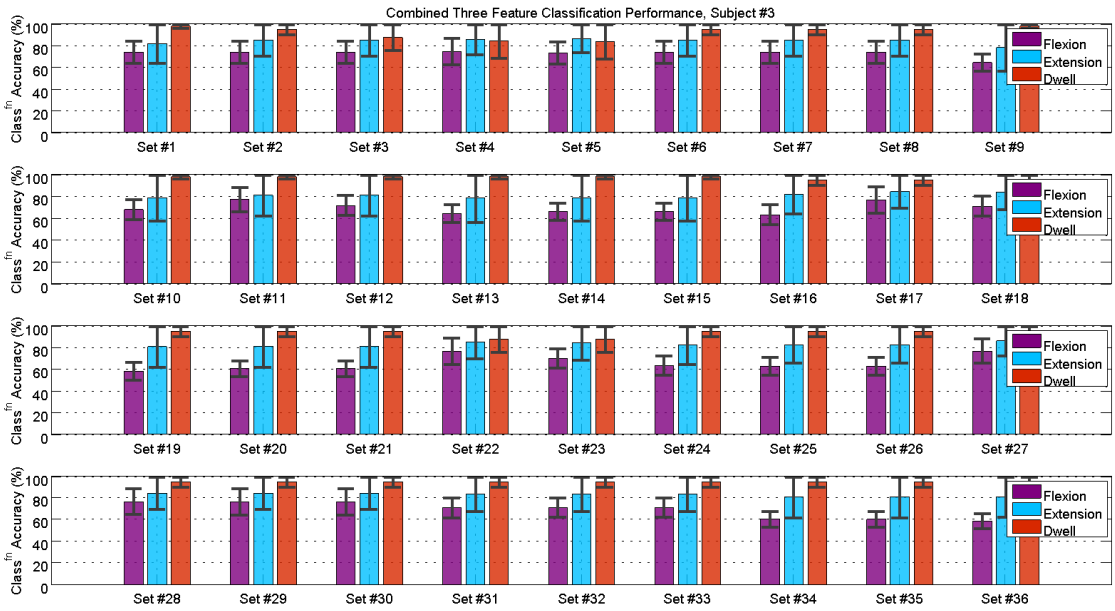

Figure 4.14: Classification performance of 3-Classifier LDA – 2 sEMG + 1 Inertial features; Subject #3.

4.2.4 Three-classifier Weighted Classifier Combination

Going back to Figures 4.3-4.8, it can be observed that all the individual features have different classification accuracies for each of the three classes. For example, knowing that feature #1 delivers 92% classification accuracy for extension but only up to 50% classification accuracy for dwell, it can be posited that feature #1 is a very reliable feature for classifying extension, but not as reliable for classifying dwell. So, this information can be taken into account while combining this feature with other features. Particularly, weights can be applied to the output of each classifier and the combination of these weighted classifiers can deliver better classification accuracy for all classes. The weights are derived from the training classification accuracy of each feature, as detailed in section 3.4.4. The weighted feature combinations with the best classification performance for the

three subjects are listed in Table 4.3, and their respective classification performance is shown in Fig. 4.15.

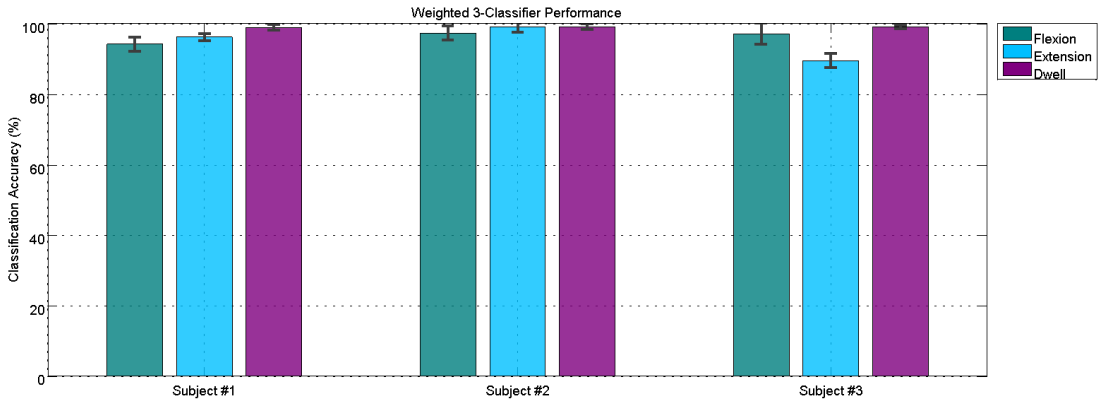

Figure 4.15: Classification performance of weighted 3-Classifier LDA.

From Fig. 4.15, we observe consistent classification accuracies for all three classes, for subjects #1 and #2, and mostly conforming classification accuracies for subject #3. While training these classifiers, it was observed that the classifiers generated from the data corresponding to slower data collection trials were generalizable and well suited to classifying all the available data. On the other hand, classifiers generated from the data corresponding to faster trials were not generalizable. This observation was further analyzed and the associated findings are illustrated in Fig. 4.16. It was found that the speed of the training activity had a bearing on the classification performance. Subsequently, the 10-fold validation procedure for evaluating classifiers was adjusted to exclude the data from the faster trials during classifier generation (training), but to include it during testing.

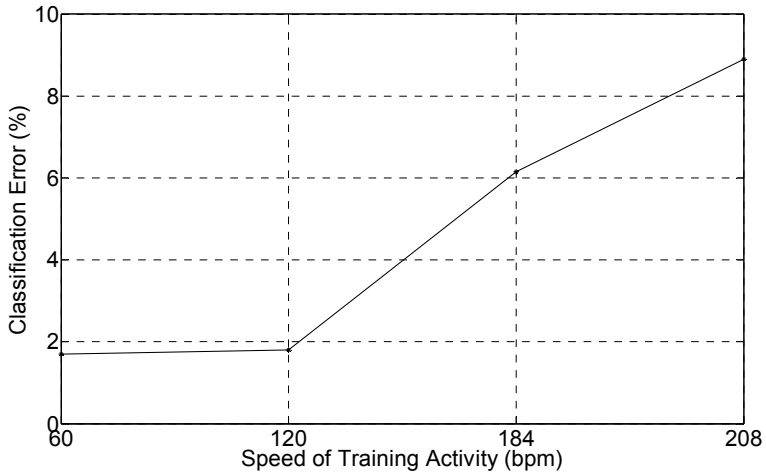

Figure 4.16: Variation of classifier performance with speed of activity used for generating classifiers.

Up to this point, the classification performance was demonstrate on partitioned chunks of data. In order to demonstrate the performance on a continuous stream of activity data that would be encountered in real-life, a weighted 3-feature classifier was tested on a 60s activity stream collected from subject #1. The performance of this classifier on the activity stream is shown in Fig 4.17.

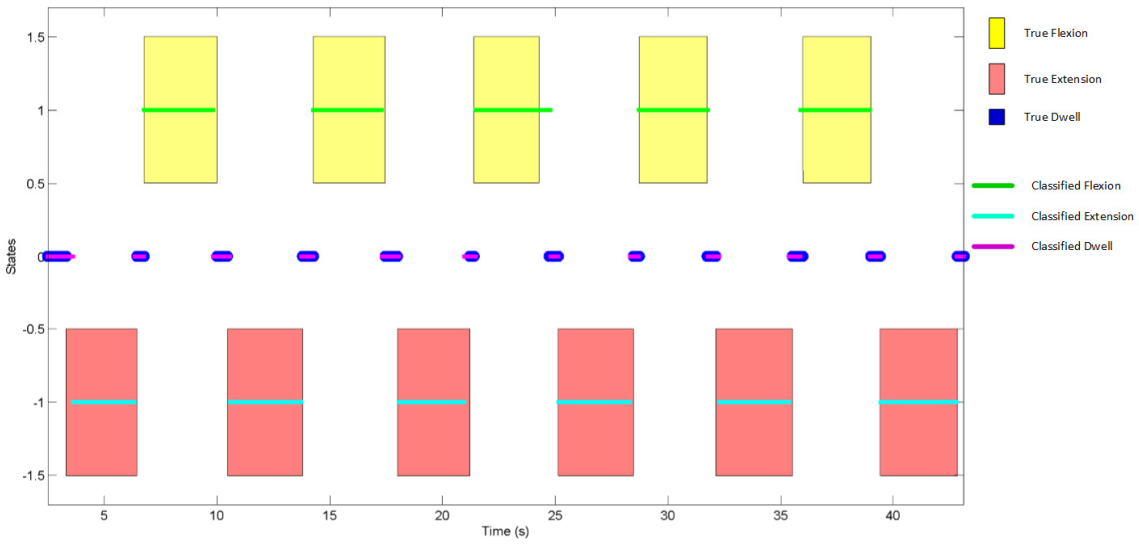

Figure 4.17: Classification performance of weighted 3-classifier LDA on continuous activity stream.

In Fig. 4.17, the three states/classes are designated numerically, such that flexion=+1, extension=-1, and dwell=0. The true states are shown in patches and the classification result is overlaid on the true states. Two major regions of misclassification can be observed just before the 25 second mark and around the 2 second mark, but mostly consistent classification is seen throughout the stream. The classification performance on this stream of data corresponded to 2% error or 98% accuracy.

4.3 Comparison with Nonlinear Classifiers

For an empirical comparison with other classification methods, three different classification algorithms with three different feature spaces, totaling to six instances were considered for evaluation. These algorithms and their associated feature spaces, parameters, and other variables are summarized here. A three-class classification was carried out in each case. The three classes were defined as a) Flexion in the sagittal plane, b) Extension in the sagittal plane, c) Dwell, or inactivity.

Multi-classifier linear discriminant analysis with time-Domain and frequency-domain features (LDA – TD+FD)

Time-domain and frequency-domain features listed in section 3.1.2 were used for classification with a multi-classifier strategy. Separate classifiers were generated from each feature, which were then combined using a majority voting method.

Multi-classifier linear discriminant analysis with time-frequency domain features (LDA – WT)

Time-frequency domain features, extracted using the wavelet transform and listed in Table 3.1 in section 3.1.2 were used for classification with a multi-classifier strategy.

Separate classifiers were generated from each feature, which were then combined using a majority voting method.

Weighted multi-classifier linear discriminant analysis with time-frequency domain features (LDA – WT + Weights)

Wavelet transform listed in Table 3.1 in section 3.1.2 were used for classification with a multi-classifier strategy. Separate classifiers were generated from each feature, which were then combined using a weighted voting method.

Support vector machines with raw data (SVM - Raw)

A support vector machine (SVM) is a powerful classification method for data that is not linearly separable. It performs non-linear classification using kernel based methods that map data very efficiently map into higher dimensions to look for separability. The LIBSVM package [83] was employed to perform a C-SVM or a generic large margin SVM. Since the SVM maps input data into higher dimensions for classification, it essentially operates as a non-linear transform on the data. So it would be interesting to see the classification performance of the method on raw input data. A radial basis function (RBF) kernel was used with a cost parameter or margin of C = 1000, and default regularization parameter.

Support vector machines with time domain and frequency domain features (SVM – TD+FD)

The same time domain and frequency domain features mentioned above in this section were used with a C-SVM classifier. A radial basis function (RBF) kernel was used with a cost parameter or margin of C = 1000, and default regularization parameter.

Support vector machines with time-frequency domain features (SVM – WT)

Time-frequency domain features, extracted using the wavelet transform and listed in section 3.2 were used for classification with a C-SVM classifier. Once again, a radial basis function (RBF) kernel was used with a cost parameter of C = 1000, and default regularization parameter.

Evaluation

The performance of the classification algorithms and feature combinations is solely quantified in terms of the classification error and classification accuracy, which were defined in the previous chapter.

The LDA classifiers report three accuracy values for the three classes, while the SVM classifier reports a single accuracy value. In order to enable comparison, the root mean square (RMS) of the three LDA reported accuracy values is calculated and used in the subsequent analysis. To evaluate classifier performance, a ten-fold cross validation method that was used in the previous chapter, is employed and the results are reported.

4.3.1 Comparison of feature domains.

In order to gauge the benefit of using time-frequency domain features we first compare the classification accuracy of a multi-classifier LDA with no weighting, using time-domain and frequency domain features, against the classification accuracy of the same classifier with time-frequency domain (wavelet domain) features. The results of the comparison for the three subjects are listed in Table 4.4 and shown graphically in Fig 4.18.

Table 4.4: Comparison of Feature Domains.

	Classification Accuracy		
	Subject #1	Subject #2	Subject #3
Wavelet Transform Features	91.3%	89.5%	85.9%
Time-Domain and Frequency-Domain	78.1%	85.2%	79.4%

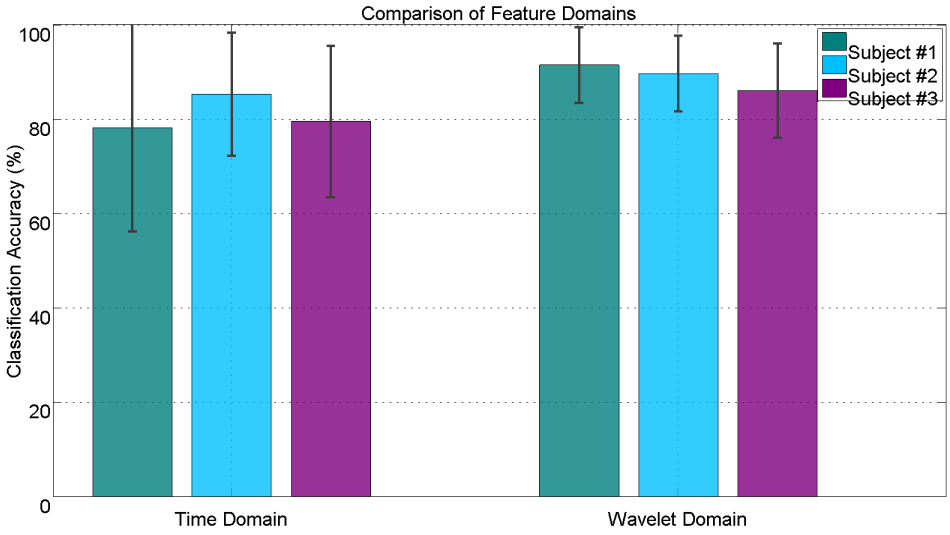

Figure 4.18: Effect of feature domain on classification performance for three subjects.

From Fig. 4.18 and from the table we can see that the use of time-frequency (wavelet) domain features leads to a 16.7% improvement in the classification accuracy for subject #1. For subjects #2 and #3, the corresponding improvement in classification accuracy is 5.1% and 8.2%, respectively. However, when viewed with respect to the classification error, the corresponding reduction in the classification error is 60.5%, 29.1% and 32% for subjects #1, #2 and #3, respectively.

4.3.2 Comparison of Classification Methods

The results of applying the methods listed in section 3.3 to the data from subject #1 are listed in Table 4.5 and illustrated in Fig. 4.19.

Table 4.5: Comparison of Classification Methods, Subject #1.

		LDA (TD+FD)	LDA (WT)	Weighted LDA (WT)	SWM (Raw Data)	SVM (TD+FD)	SVM (WT)
Classification Accuracy	Mean	78.1%	91%	97.5%	78.5%	42.3%	94%
	Standard Deviation	22%	8%	1.4%	5.7%	7%	4.2%

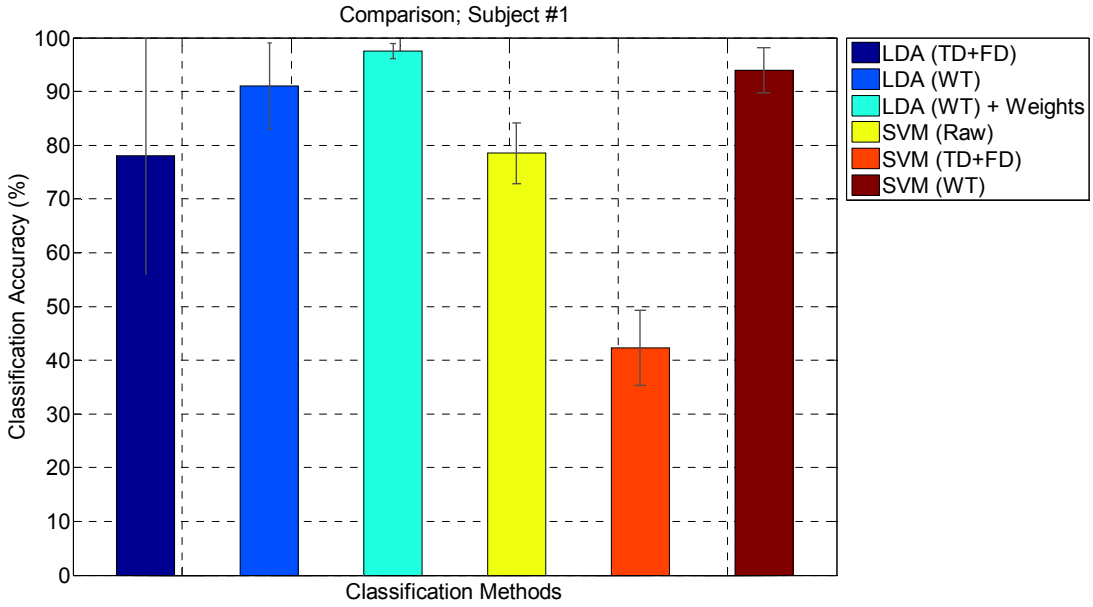

Figure 4.19: Comparison of classification methods, Subject #1.

From Fig. 4.19 and Table 9, the first observation that can be made is the 16.7% improvement in classification accuracy as a result of using wavelet domain features with multi-classifier LDA, which was mentioned in the previous analysis. We also see that a finely tuned, weighted multi-classifier LDA with wavelet domain features delivers an additional 7% improvement in classification accuracy. Additionally, it can also be observed that SVM with wavelet domain features (SVM-WT) delivers better performance than multi-classifier LDA with wavelet domain features (LDA-WT), and comparable performance to weighted multi-classifier LDA with wavelet domain features (LDA-WT-weights). It is necessary to point out that a SVM with wavelet domain features (SVM-WT)

essentially performs two successive non-linear transforms on the data: first with wavelet transform feature extraction and subsequently with SVM. On the other hand, multi-classifier LDA with wavelet domain features (LDA-WT) consists of a single transform operation followed by classification.

It can also be observed that the performance of SVM with raw data is comparable to the performance of LDA with time-domain and frequency-domain features. This points to the ability of SVM to seek maximal separation between classes in a dataset. In addition, it can also be observed that using time-domain and frequency-domain features with SVM delivers an unexpected drop in performance. It is possible that discriminating properties in the features get averaged out due to feature extraction and transform operations during SVM. This behavior could be further studied through additional investigation of feature properties. It is also possible that a different cost parameter and regularization parameter might have led to better performance. However, the same parameters were used throughout to enable better comparison. A similar analysis was carried out on data from subjects #2 and #3, and the results are listed in Tables 4.6 and 4.7, and illustrated in Figures 4.20 and 4.21.

Table 4.6: Comparison of Classification Methods, Subject #2.

		LDA (TD+FD)	LDA (WT)	Weighted LDA (WT)	SVM (Raw Data)	SVM (TD+FD)	SVM (WT)
Classification Accuracy	Mean	85.1%	89%	96.9%	87.65%	47.4%	96%
	Standard Deviation	13%	8%	1.5%	3.1%	7%	4.2%

Table 4.7: Comparison of Classification Methods, Subject #3.

		LDA (TD+FD)	LDA (WT)	Weighted LDA (WT)	SWM (Raw Data)	SVM (TD+FD)	SVM (WT)
Classification Accuracy	Mean	79%	86%	94.7%	85.6%	50.7%	95%
	Standard Deviation	16%	10%	2.6%	5.1%	5%	2.9%

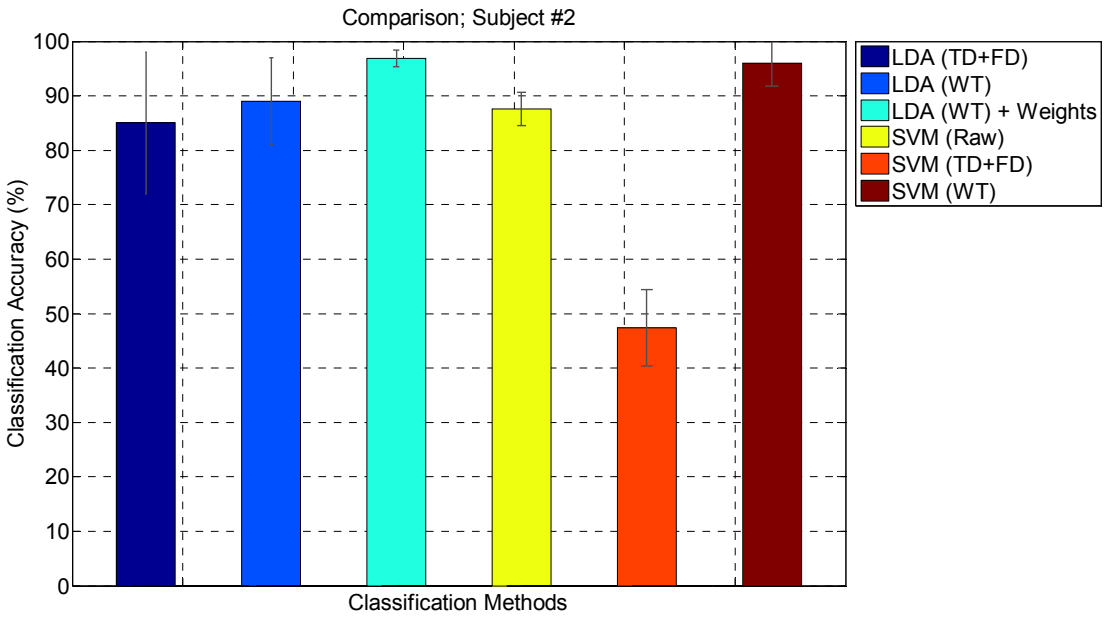

Figure 4.20: Comparison of classification methods, Subject #2.

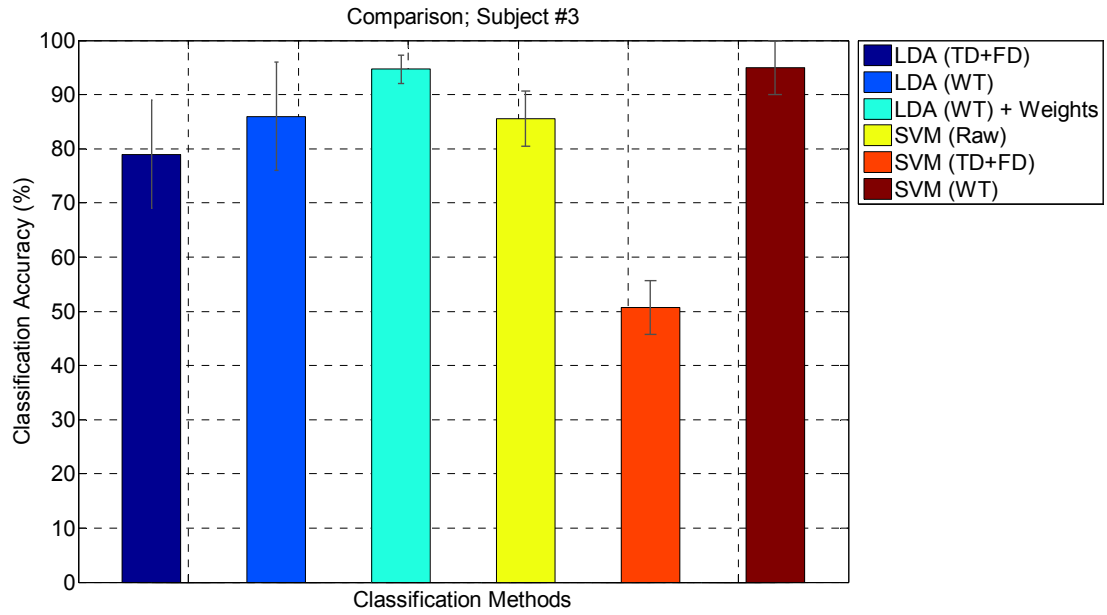

Figure 4.21: Comparison of classification methods, Subject #3.

The same general trends that were observable in Fig. 4.19, can also be observed in Figures 4.20 and 4.21. Improvement in classification accuracy as a result of using wavelet

domain features with multi-classifier LDA can be seen to be 5.1% and 8.2% for subjects #2 and #3, respectively. A further 8%-10% improvement in classification accuracy owing to the use of a finely tuned, weighted multi-classifier LDA with wavelet domain features is also observed.

From Figures 4.19-4.21, it can also be observed that SVM with raw data delivers classification performance that is better than LDA with time-domain and frequency-domain features (LDA-TD+FD), and comparable to multi-classifier LDA with wavelet domain features (LDA-WT). Additionally, it can also be observed that SVM with wavelet domain features (SVM-WT) delivers far better performance than multi-classifier LDA with wavelet domain features (LDA-WT), and comparable performance to weighted multi-classifier LDA with wavelet domain features (LDA-WT-weights).

4.4 Chapter Summary

A multi-sensor, multi-classifier approach for recognizing user intent in performing activity and evaluated for classification accuracy. It was demonstrated that the multi-classifier approach is up to 16% more accurate than a single classifier approach. In addition, a method of weighted classifier combination, to collaboratively improve classification accuracy was also demonstrated. Results show that 3-classifier setup with two sEMG features and 1 inertial feature can deliver up to 98% accuracy in classifying flexion and extension motion of the torso in the sagittal plane.

Additionally, an empirical comparison between six methods of classification was presented. The six methods were multi-classifier LDA using time-domain and frequency-domain features, multi-classifier LDA using time-frequency domain features, weighted multi-classifier LDA using time-frequency domain features, SVM using raw data, SVM

using time-domain and frequency-domain features, and SVM using time-frequency domain features. Results of the comparison showed that the use of time-frequency domain features with LDA led to a 30%-60% drop in classification error, when compared to LDA using time-domain and frequency-domain features. The comparison also showed that a weighted, multi-classifier LDA using time-frequency domain features delivered numerically similar accuracy as a nonlinear SVM classifier using time-frequency domain features.

CHAPTER 5

CONCLUSION AND FUTURE DIRECTIONS

This research effort was premised as an exploration of the space between linear and non-linear methods of classification. Specifically, the use of non-linear features with linear methods of classification was investigated for classification accuracy comparable to non-linear methods of classification. This investigation was driven by the impetus to avoid negative aspects of non-linear classification methods such as computational complexity and susceptibility to noise and overfitting.

Over the course of the dissertation, it was demonstrated that the use of non-linear features, specifically time-frequency domain features with linear discriminant analysis (LDA) based methods of classification leads to substantial reduction in classification error. Moreover, it was also demonstrated that combination of multiple classifiers, coupled with time-frequency domain features delivers classification accuracy comparable to more powerful non-linear methods of classification.

The methods presented here have enabled accurate and computationally efficient intent recognition of torso movements. This is important for assistive device applications for the back and upper-body. An accurate and efficient method of intent recognition will provide a means to the design of human interface and control systems for such devices which is the motivation for this work. Biomechanics simulations to understand the interaction between external objects and the human body are a major part of the design of an assistive device that provided the motivation for this dissertation. The outputs of the presented classifiers can be directly used as control inputs instead of muscle activations from a model, to simulate the operation of an external device in simulation.

More broadly, the research presented could be extended to benefit human health in other applications. The combination of sEMG and inertial signals, coupled with a pattern classification methodology make it possible to design systems to interpret the outputs of the presented classifiers to recognize muscle spasms or even detect events that would contribute to a fall for a user. Moreover, the presented classification method could be extended to help with physical therapy or sports training for upper body movements.

Immediate next steps that could be addressed to continue this research are presented here and would increase the number of recognized classes, move the system to real-time, and improve the training of the classifiers.

1) Extension of the current classifier to classify additional motion such as twisting and lateral bending. It is hypothesized that the multi-classifier combination approach will be useful in this case.
2) Real-time implementation of multi-classifier approach. The current implementation is a post-processing implementation. However, it has been geared so that it can be implemented in real-time with minimal effort. Wavelet transform feature extraction has been intentionally implemented in a dyadic framework, so that real-time implementation can be accomplished either by employing the Fast Wavelet Transform, which is based on the famous Cooley-Tukey algorithm, or discrete wavelet transform filters.
3) On-line training through adoption of adaptive-LDA [84]. Currently training of classifiers consumes a lot of time and is not suited for on-line or field training. An adaptive-LDA based approach can help implement on-line training.

While working on this dissertation, a number of open research questions were encountered, which have not been addressed in the body of the dissertation. These open questions and the possibilities they entail are briefly discussed here.

1) Surface EMG signals display a lot of variation when the muscles in question are under fatigue. While an attempt was made to collect data over multiple successive trials, it is not enough to account for fatigue. Training a classifier that can detect fatigue is therefore an interesting open question.
2) The classifiers discussed in this dissertation deliver real-time intent in terms of one of three activities – flexion, extension and dwell. However, in the current state the classifiers do not have an ability to provide any information about the intensity or amplitude of the intended motion. This is currently an open question, but it should be possible to train a future classifier using the framework presented in this dissertation to deliver intensity or amplitude as an output.
3) The classifiers presented in this study were trained on data collected in a controlled environment only. No additional tests were conducted to determine the robustness of the classifiers. It is expected that these classifiers will behave differently when subject to environmental conditions such as heat, humidity, external motion, etc. and the design of robust classifiers is an interesting challenge.
4) Continuing with the idea of robustness, quantifying the sensitivity of a classifier to variations in sensor location, to account for errors or subjectivity while mounting sensors is another avenue for investigation.

5) On the same theme, quantifying sEMG electrode reliability so that the classifier can intelligently understand when an electrode comes loose can possibly be addressed in the future.
6) It is well known that the performance of classifiers generally degrades over time as newer data is encountered and eventually re-training becomes necessary. These conditions were not encountered while working on this dissertation so this is an unaddressed topic of inquiry.
7) A possibility of a global classifier is also an open question. The classifiers in this study were entirely local – a separate classifier was designed for every subject. However, a global classifier that approximately represents a population, in conjunction with a locally trained classifier would be interesting from the perspective of fast training.
8) Deep learning methods such as convolutional neural networks (CNNs) have made a significant impact on machine learning applications in the recent past. Now that dedicated hardware for CNNs is becoming commercially available, it might be interesting to explore this approach.

APPENDIX A

PROTOCOL OF EXPERIMENTS

Purpose:

It has been proposed that a combination of sEMG and inertial sensors can provide sufficient information to recognize the intent of a person wearing a spine exoskeleton. This study aims to evaluate the performance of these two signals in recognizing intent.

Materials:

1) High speed motion capture system – Qualisys Oqus.
2) EMG measurement system – Delsys Myomonitor IV.
3) Reflective markers – 16 mm diameter.
4) Planar marker clusters.
5) Adhesive tapes, dots and bandages.
6) Alcohol wipes.

Method:

1) Calibrate camera system - place L-frame to coincide with markings on force plate.
2) Explain experiment to and obtain informed consent from test participant.
3) Measure participant's height and weight. Record age and gender.
4) Locate and mark C7, T4, T7, L1 vertebrae through palpation of the participant's back.
5) Identify sEMG sites – erector spinae at L1, L3, T9, rectus abdominis, obliques.
6) Prepare skin for application of sEMG sensors using sandpaper and alcohol wipes.

7) Test and ensure output from every electrode on Delsys EMG screen. If required, detach and reapply.
8) Apply reflective markers on participant's body, at prominent anatomical locations enumerated in the list of markers.
9) Using 'fabrifoam' wrap and skin adhesive, carefully affix marker-clusters to segments defined by the markers on the back.
10) Ensure that motion capture (240 Hz) and EMG recording (1200 Hz) are synchronized.
11) Zero the force plate (calibration with no load).
12) Capture 5 seconds of baseline data, with participant away from force platform. Ensure that data has been recorded.
13) Ask participant to stand facing wall, perpendicular to shorter arm of the L-frame.
14) Ask participant to perform following motions in order. After every 10th motion is completed, ask participant if he/she needs rest, water.
    i. Stand in neutral position – 15 s
    ii. Twist torso left and back to neutral position – 40 bpm – 60 s
    iii. Twist torso right and back to neutral position – 40 bpm – 60 s
    iv. Stand in neutral position – 10 s
    v. Twist torso left and back to neutral position – 60 bpm – 60 s
    vi. Twist torso right and back to neutral position – 60 bpm – 60 s
    vii. Stand in neutral position – 10 s
    viii. Twist torso left and back to neutral position – 120 bpm – 60 s
    ix. Twist torso right and back to neutral position – 120 bpm – 60 s
    x. Stand in neutral position – 10 s
    xi. Twist torso left and back to neutral position – 184 bpm – 60 s
    xii. Twist torso right and back to neutral position – 184 bpm – 60 s
    xiii. Stand in neutral position – 10 s
    xiv. Twist torso left and back to neutral position – 208 bpm – 30 s

xv. Twist torso right and back to neutral position – 208 bpm – 30 s

xvi. Stand in neutral position – 10 s

xvii. Flexion/Extension – Bend forward and stand back up – 60 bpm – 60 s

xviii. Flexion/Extension – Bend forward and stand back up – 92 bpm – 60 s

xix. Flexion/Extension – Bend forward and stand back up – 120 bpm – 60 s

xx. Stand in neutral position – 10 s

xxi. Flexion/Extension – Bend forward and stand back up – 152 bpm – 60 s

xxii. Flexion/Extension – Bend forward and stand back up – 184 bpm – 60 s

xxiii. Flexion/Extension – Bend forward and stand back up – 208 bpm – 60 s

xxiv. Stand in neutral position – 10 s

xxv. Twist torso left and hold position – 30 s

xxvi. Twist torso right and hold position – 30 s

xxvii. Stand in neutral position – 10 s

xxviii. Hold flexed position – Bend forward roughly 30° and hold position for 30 s. (return to neutral position)

xxix. Hold flexed position – Bend forward roughly 60° and hold position for 30 s. (return to neutral position)

xxx. Hold extended position – Hyper-extend roughly 5° and hold position for 30 s. (return to neutral position)

xxxi. Hold extended position – Hyper-extend roughly 15° (as far as possible) and hold position for 30 s. (return to neutral position)

xxxii. Stand in neutral position – 10 s

15) Detach EMG system, electrodes and markers from participant's body.

APPENDIX B

TWO-CLASS CLASSIFICATION

An exploratory analysis with a two-class LDA, using single all-encompassing classifiers was carried out on experimentally recorded biomechanical signals. Segments of the signals, corresponding to the commencement and conclusion of each activity (flexion and extension) were isolated into separate databases. These two databases corresponded to the two classes of interest. Three sets of such a pair of databases were created. These sets were 1) Database-pair of only sEMG signals – 12 data streams per database; 2) Database-pair of only inertial signals – 20 data streams per database; 3) Database-pair of combined sEMG and inertial signals – 32 data streams per database. These database-pairs were split into two sets. The first set of each database-pair was designated the 'training set'. This was made up of data from that corresponded to 73% of all the collected data points. The training sets were used to generate classifiers, according to (5)-(10). The second set was designated the 'test set'. This was made up of trials independent from those used for generating classifiers and comprised of data that corresponded to 27% of all the collected data points. The test sets were used to validate the classifiers generated by the training sets. The training sets of the three database-pairs were stacked together and a 2-class linear discriminant analysis was conducted on each pair. The classifiers generated by this analysis were validated against the test sets. The results so obtained help us compare and evaluate the classification performance of a multi-sensor fusion approach against a single sensor approach.

The classification performance of the database-pair of only sEMG signals, is illustrated in Fig. B.1(a, b). Fig. B.1(a) shows the mapped, feature space, after classification. The dimensions of the mapped feature space correspond to the number of classes, reduced by 1. A 2-class linear discriminant analysis therefore, results in a one-dimensional feature space, as can be seen in the same figure. The figure also shows a discriminant line, demarcating the boundaries of the two classes. The graph on the right in Fig. B.1(a) shows the corresponding probability distribution of the mapped feature space. The probability distribution indicates the spread of the two classes. In this case, we see a prominent overlap between the two classes, indicating that the classifier generated from the database-pair of sEMG signals is prone to error. This error in classification was calculated for the two classes, and the results are listed in Table B.1.

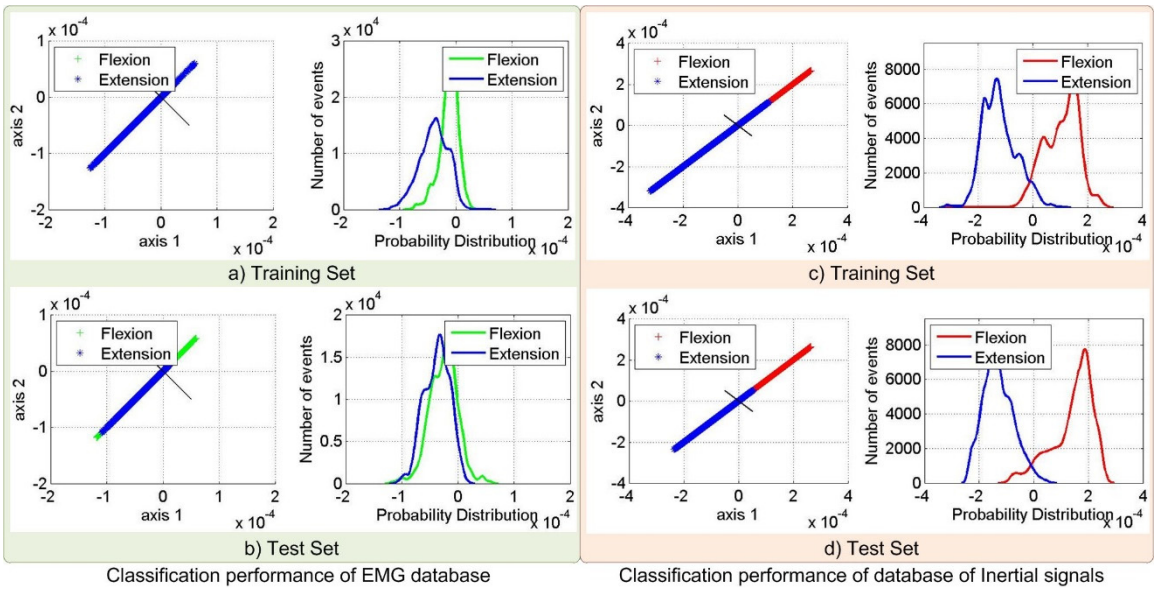

Figure B.1: Two-class classification performance of separate sEMG signals and inertial signals.

Table B.1: Two-class Classification; sEMG signals.

Class	**Classification Error**	
	Training Data	Test Data
Flexion	77.5 %	86.4 %
Extension	4.0 %	3.7 %

From the table, we see that the classifier generated from the database-pair of only EMG signals, fails to classify flexion. The performance of the classifier on the 'test set' of sEMG signals is also listed in Table B.1, and shown in Fig. B.1(b). We see a performance similar to that of the training set, without any significant change in the error.

The classification performance of the database-pair of only inertial signals, is depicted in Fig. B.1(c). Similar to Fig. B.1(a), we see the one-dimensional, mapped feature space, after classification, and the discriminant line delineating the two classes in Fig. B.1(c). Also shown is the corresponding probability distribution of the mapped feature space. In this case, we see an improved separation between the two classes, with some overlap. The error corresponding to the overlap was calculated for the two classes, and the results are listed in Table B.2.

Table B.2: Two-class Classification; Inertial signals.

Class	**Classification Error**	
	Training Data	Test Data
Flexion	5.6 %	5.9 %
Extension	4.0 %	1.8 %

We see an improvement in classification performance, for flexion. The performance of the classifier on the 'test set' of inertial signals is also listed in Table B.2, and shown in Fig. B.1(d). We see a performance similar to that of the training set, validating the performance of the classifier.

The classification performance of the database-pair of combined sEMG and inertial signals, is shown in Fig. B.2(a). We see a similar separation between the two classes. The error corresponding to the overlap for the two classes is listed in Table B.3. We see that the combined database-pair delivers the best classification performance for extension, but sub-optimal classification for flexion.

Table B.3: Two-class Classification; Combined sEMG and Inertial signals.

Class	**Classification Error**	
	Training Data	Test Data
Flexion	8.5 %	11.9 %
Extension	1.3 %	0.6 %

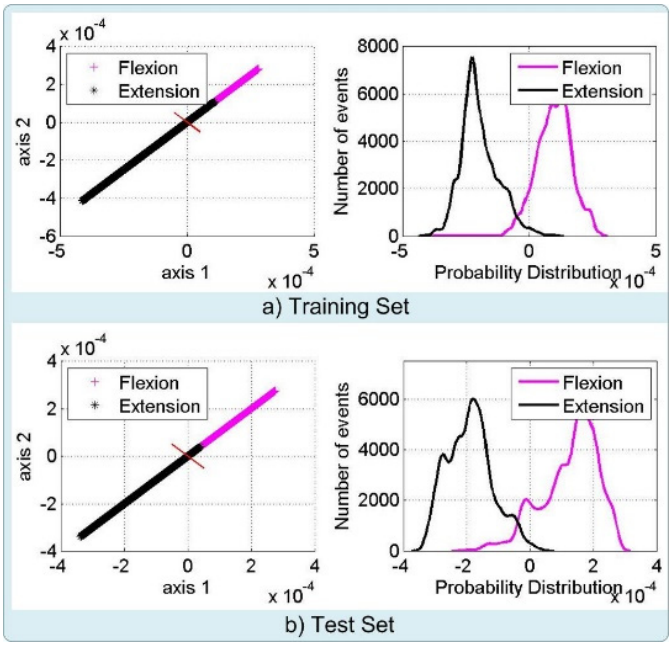

Figure B.2: Two-class classification performance of combined sEMG and inertial signals.

The performance of the classifier generated from the combined database on the corresponding ‘test set’ is also listed in Table B.3, and shown in Fig. B.2(b). The classification performance on the test set is similar to that of the training set.

The major takeaway from this analysis was that it was possible to improve classification accuracy by utilizing a multi-sensor classification approach.

REFERENCES

[1] G. Sukthankar, C. Geib, H. Hai Bui, D. Pynadath, and R. Goldman, *Plan, Activity, and Intent Recognition: Theory and Practice*. Morgan Kaufmann Publishers, 2014.

[2] A. M. Simon, K. A. Ingraham, J. A. Spanias, A. J. Young, and L. J. Hargrove, "Development and preliminary testing of a flexible control system for powered knee-ankle prostheses," in *2016 6th IEEE International Conference on Biomedical Robotics and Biomechatronics (BioRob)*, 2016, pp. 704–709.

[3] H. Z. Hao, J. Reher, J. Horn, V. Paredes, and A. D. Ames, "Realization of stair ascent and motion transitions on prostheses utilizing optimization-based control and intent recognition," *IEEE International Conference on Rehabilitation Robotics*, vol. 2015-Septe, pp. 265–270, 2015.

[4] A. J. Young, T. A. Kuiken, and L. J. Hargrove, "Analysis of using EMG and mechanical sensors to enhance intent recognition in powered lower limb prostheses.," *Journal of neural engineering*, vol. 11, no. 5, p. 056021, 2014.

[5] H. A. Varol, F. Sup, and M. Goldfarb, "Multiclass real-time intent recognition of a powered lower limb prosthesis," *IEEE Transactions on Biomedical Engineering*, vol. 57, no. 3, pp. 542–551, 2010.

[6] A. Young and L. Hargrove, "A Classification Method for User-Independent Intent Recognition for Transfemoral Amputees Using Powered Lower Limb Prostheses," *IEEE Transactions on Neural Systems and Rehabilitation Engineering*, vol. 4320, no. c, pp. 1–1, 2015.

[7] R. O. Duda, P. E. Hart, and D. G. Stork, *Pattern Classification*. New York: Wiley, 2001.

[8] Y. S. Abu-Mostafa, M. Magdon-Ismail, and H.-T. Lin, *Learning from Data: A Short Course*. United States: AMLBook, 2012.

[9] H. Zhang, A. Kadrolkar, and F. C. Sup, "Design and Preliminary Evaluation of a Passive Spine Exoskeleton," *Journal of Medical Devices*, vol. 10, no. 1, p. 011002, 2015.

[10] K. Moore and A. Dalley, *Clinically Oriented Anatomy*. Philadelphia: Lippincott Williams & Wilkins, 1999.

[11] D. Allbrook, "Movements of the Lumbar Spinal Column," *The Journal of Bone and Joint Surgery*, vol. 39-B, no. 2, pp. 339–345, May 1957.

[12] A. Bergmark, "Stability of the Lumbar Spine: A study in mechanical engineering," *Acta orthopaedica Scandinavica*, vol. 60, no. 230, pp. 1–54, 1989.

[13] E. Criswell and J. Cram, *Cram's Introduction to Surface Electromyography*. Sudbury, MA: Jones and Bartlett, 2011.

[14] T. B. Belytschko, T. P. Andriacchi, A. B. Schultz, and J. O. Galante, "Analog studies of forces in the human spine: Computational techniques," *Journal of Biomechanics*, vol. 6, no. 4, pp. 361–371, Jul. 1973.

[15] T. Andriacchi, A. Schultz, T. Belytschko, and J. O. Galante, "A model for studies

of mechanical interactions between the human spine and rib cage," *Journal of Biomechanics*, vol. 7, no. 6, pp. 497–507, Nov. 1974.

[16] G. Kamen and D. A. Gabriel, *Essentials of Electromyography*. Human Kinetics, 2010.

[17] W. F. Brown, *The Physiological and Technical basis of Electromyography*. Boston: Butterworths, 1984.

[18] D. Farina, R. Merletti, and R. M. Enoka, "The extraction of neural strategies from the surface EMG.," *Journal of Applied Physiology*, vol. 96, no. 4, pp. 1486–1495, Apr. 2004.

[19] D. Farina, M. Gazzoni, and R. Merletti, "Assessment of low back muscle fatigue by surface EMG signal analysis: methodological aspects," *Journal of Electromyography and Kinesiology*, vol. 13, no. 4, pp. 319–332, Aug. 2003.

[20] J. L. G. Nielsen, S. Holmgaard, N. Jiang, K. B. Englehart, D. Farina, and P. A. Parker, "Simultaneous and proportional force estimation for multifunction myoelectric prostheses using mirrored bilateral training.," *IEEE transactions on bio-medical engineering*, vol. 58, no. 3, pp. 681–688, Mar. 2011.

[21] M. H. Pope, A. Aleksiev, N. D. Panagiotacopulos, J. S. Lee, D. G. Wilder, K. Friesen, W. Stielau, and V. K. Goel, "Evaluation of Low Back Muscle Surface EMG Signals using Wavelets," *Clinical Biomechanics*, vol. 15, no. 8, pp. 567–573, Oct. 2000.

[22] Y. Bastiaensen, T. Schaeps, and J. Baeyens, "Analyzing an sEMG signal using wavelets," *4th European Conference of the International Federation for Medical and Biological Engineering*, vol. 22, no. 6, pp. 156–159, Jan. 2009.

[23] P. S. Addison, *The Illustrated Wavelet Transform Handbook : Introductory Theory and Applications in Science, Engineering, Medicine, and Finance*. Bristol, UK; Philadelphia: Institute of Physics Pub., 2002.

[24] C. S. Pattichis and M. S. Pattichis, "Time-scale analysis of motor unit action potentials.," *IEEE Transactions on Bio-Medical Engineering*, vol. 46, no. 11, pp. 1320–1329, Nov. 1999.

[25] D. Zennaro, P. Wellig, V. M. Koch, G. S. Moschytz, and T. Läubli, "A Software Package for the Decomposition of Long-Term Multichannel EMG Signals using Wavelet Coefficients.," *IEEE Transactions on Bio-Medical Engineering*, vol. 50, no. 1, pp. 58–69, Jan. 2003.

[26] L. Peeraer, B. Aeyels, and G. Van der Perre, "Development of EMG-based mode and intent recognition algorithms for a computer-controlled above-knee prosthesis," *Journal of Biomedical Engineering*, vol. 12, no. 3, pp. 178–182, May 1990.

[27] K. H. Ha, H. A. Varol, and M. Goldfarb, "Volitional control of a prosthetic knee using surface electromyography.," *IEEE transactions on bio-medical engineering*, vol. 58, no. 1, pp. 144–51, Jan. 2011.

[28] N. Jiang, K. B. Englehart, and P. A. Parker, "Extracting simultaneous and

proportional neural control information for multiple-DOF prostheses from the surface electromyographic signal.," *IEEE transactions on bio-medical engineering*, vol. 56, no. 4, pp. 1070–1080, Apr. 2009.

[29] K. Englehart, B. Hudgins, and P. A. Parker, "Time-frequency based classification of the myoelectric signal: static vs. dynamic contractions," in *Proceedings of the 22nd Annual International Conference of the IEEE Engineering in Medicine and Biology Society*, 2000, vol. 1, pp. 317–320.

[30] F. Tenore, R. S. Armiger, R. J. Vogelstein, D. S. Wenstrand, S. D. Harshbarger, and K. Englehart, "An embedded controller for a 7-degree of freedom prosthetic arm.," *30th Annual International Conference of the IEEE Engineering in Medicine and Biology Society*, pp. 185–188, Jan. 2008.

[31] E. J. Vos, M. G. Mullender, and G. J. van Ingen Schenau, "Electromechanical delay in the vastus lateralis muscle during dynamic isometric contractions," *European Journal of Applied Physiology and Occupational Physiology*, vol. 60, no. 6, pp. 467–471, Nov. 1990.

[32] E. J. Vos, J. Harlaar, and G. J. van Ingen Schenau, "Electromechanical delay during knee extensor contractions.," *Medicine and science in sports and exercise*, vol. 23, no. 10, pp. 1187–93, Oct. 1991.

[33] E. M. Winter and F. B. C. Brookes, "Electromechanical response times and muscle elasticity in men and women," *European Journal of Applied Physiology and Occupational Physiology*, vol. 63, no. 2, pp. 124–128, Aug. 1991.

[34] K. Englehart, B. Hudgins, P. . Parker, and M. Stevenson, "Classification of the Myoelectric Signal using Time-Frequency based Representations," *Medical Engineering & Physics*, vol. 21, no. 6–7, pp. 431–438, Jul. 1999.

[35] M.-F. Lucas, A. Gaufriau, S. Pascual, C. Doncarli, and D. Farina, "Multi-channel surface EMG classification using support vector machines and signal-based wavelet optimization," *Biomedical Signal Processing and Control*, vol. 3, no. 2, pp. 169–174, Apr. 2008.

[36] K. Yamamoto, M. Ishii, H. Noborisaka, and K. Hyodo, "Stand alone wearable power assisting suit - sensing and control systems," in *Proceedings of the 3th IEEE International Workshop on Robot and Human Interactive Communication, ROMAN*, 2004, pp. 661–666.

[37] K. Naruse, S. Kawai, H. Yokoi, and Y. Kakazu, "Design of Wearable Power-Assist Device for Lower Back Support," *Journal of Robotics and Mechatronics*, vol. 16, no. 5, pp. 489–496, 2004.

[38] K. Naruse, S. Kawai, H. Yokoi, and Y. Kakazu, "Development of wearable exoskeleton power assist system for lower back support," in *Proceedings of the IEEE/RSJ International Conference on Intelligent Robots and Systems*, 2003, no. October, pp. 3630–3635.

[39] T. Koyama, M. Q. Feng, and T. Tanaka, "Mechanical Modeling and Control of Wearable Nursing Care Robot," in *Proc. of The Int. Conf. on Rehabilitation Robotics (ICORR2001)(M. Mokhtari (Ed.): Assistive Technology Research Series*

9), 2001, pp. 227–234.

[40] X. Li, T. Noritsugu, M. Takaiwa, and D. Sasaki, "Design of Wearable Power Assist Wear for Low Back Support Using Pneumatic Actuators," *International Journal of Automation Technology*, vol. 7, no. 2, pp. 228–236, 2013.

[41] K. Yamamoto, K. Hyodo, M. Ishii, and T. Matsuo, "Development of Power Assisting Suit for Assisting Nurse Labor.," *JSME International Journal Series C*, vol. 45, no. 3, pp. 703–711, 2002.

[42] S. Kawai, K. Naruse, H. Yokoi, and Y. Kakazu, "An Analysis of Human Motion for Control of a Wearable Power Assist System," *Journal of Robotics and Mechatronics*, vol. 16, no. 3, pp. 1–8, 2004.

[43] S. Kawai, K. Naruse, H. Yokoi, and Y. Kakazu, "A study for control of a power assist device," in *Proceedings of the IEEE/RSJ International Conference on Intelligent Robots and Systems*, 2004, vol. 3, pp. 2283–2288.

[44] M. Ishii, K. Yamamoto, and K. Hyodo, "Stand-alone wearable power assist suit-development and availability," *Journal of Robotics and Mechatronics*, vol. 17, no. 5, pp. 575–583, 2005.

[45] A. J. Young, L. H. Smith, E. J. Rouse, and L. J. Hargrove, "Classification of simultaneous movements using surface EMG pattern recognition," *IEEE Transactions on Biomedical Engineering*, vol. 60, no. 5, pp. 1250–1258, 2013.

[46] H. Huang, F. Zhang, L. J. Hargrove, Z. Dou, D. R. Rogers, and K. B. Englehart, "Continuous locomotion-mode identification for prosthetic legs based on neuromuscular-mechanical fusion.," *IEEE Transactions on Bio-medical Engineering*, vol. 58, no. 10, pp. 2867–2875, Oct. 2011.

[47] A. Chan and K. Englehart, "Continuous classification of myoelectric signals for powered prostheses using gaussian mixture models," in *Proceedings of the 25th Annual International Conference of the IEEE Engineering in Medicine and Biology Society*, 2003, pp. 2841–2844.

[48] L. J. Hargrove, G. Li, K. B. Englehart, and B. S. Hudgins, "Principal components analysis preprocessing for improved classification accuracies in pattern-recognition-based myoelectric control.," *IEEE transactions on bio-medical engineering*, vol. 56, no. 5, pp. 1407–1414, May 2009.

[49] K. Englehart, B. Hudgins, and P. A. Parker, "A Wavelet-based Continuous Classification Scheme for Multifunction Myoelectric Control," *IEEE Transactions on Biomedical Engineering*, vol. 48, no. 3, pp. 302–311, Mar. 2001.

[50] P. Parker, K. Englehart, and B. Hudgins, "Myoelectric Signal Processing for Control of Powered Limb Prostheses," *Journal of Electromyography and Kinesiology*, vol. 16, no. 6, pp. 541–548, Dec. 2006.

[51] Y. David Li and E. T. Hsiao-Wecksler, "Gait mode recognition and control for a portable-powered ankle-foot orthosis," *IEEE International Conference on Rehabilitation Robotics*, 2013.

[52] E. Scheme, A. Fougner, Stavdahl, A. D. C. Chan, and K. Englehart, "Examining

the adverse effects of limb position on pattern recognition based myoelectric control," *2010 Annual International Conference of the IEEE Engineering in Medicine and Biology Society, EMBC'10*, pp. 6337–6340, 2010.

[53] A. Kadrolkar and F. Sup, "Classification of Trunk Motion for a Backbone Exoskeleton Using Inertial Data and Surface Electromyography," in *Proceedings of the IEEE International Conference on Systems, Man, and Cybernetics*, 2013, pp. 3978–3983.

[54] N. B. N. Bu, M. Okamoto, and T. Tsuji, "A Hybrid Motion Classification Approach for EMG-Based Human-Robot Interfaces Using Bayesian and Neural Networks," *IEEE Transactions on Robotics*, vol. 25, no. 3, pp. 502–511, 2009.

[55] R. N. Khushaba, S. Kodagoda, M. Takruri, and G. Dissanayake, "Toward improved control of prosthetic fingers using surface electromyogram (EMG) signals," *Expert Systems with Applications*, vol. 39, no. 12, pp. 10731–10738, 2012.

[56] J. Chu, I. Moon, Y. Lee, S.-K. Kim, and M.-S. Mun, "A Supervised Feature-Projection-Based Real-Time EMG Pattern Recognition for Multifunction Myoelectric Hand Control," *IEEE/ASME Transactions on Mechatronics*, vol. 12, no. 3, pp. 282–290, Jun. 2007.

[57] P. Kaufmann, K. Englehart, and M. Platzner, "Fluctuating emg signals: investigating long-term effects of pattern matching algorithms.," in *International Conference of the IEEE Engineering in Medicine and Biology Society*, 2010, vol. 2010, pp. 6357–6360.

[58] A. Alkan and M. Günay, "Identification of EMG signals using discriminant analysis and SVM classifier," *Expert Systems with Applications*, vol. 39, no. 1, pp. 44–47, 2012.

[59] G. Wang, Z. Wang, W. Chen, and J. Zhuang, "Classification of Surface EMG Signals using Optimal Wavelet Packet Method based on Davies-Bouldin Criterion," *Medical & Biological Engineering & Computing*, vol. 44, no. 10, pp. 865–872, Sep. 2006.

[60] S. Au, M. Berniker, and H. Herr, "Powered ankle-foot prosthesis to assist level-ground and stair-descent gaits.," *Neural networks : the official journal of the International Neural Network Society*, vol. 21, no. 4, pp. 654–66, May 2008.

[61] L. I. Kuncheva, *Combining Pattern Classifiers: Methods and Algorithms*. Wiley, 2004.

[62] a. Phinyomark, C. Limsakul, and P. Phukpattaranont, "Application of Wavelet Analysis in EMG Feature Extraction for Pattern Classification," *Measurement Science Review*, vol. 11, no. 2, pp. 45–52, Jan. 2011.

[63] M. Flanders, "Choosing a Wavelet for Single-Trial EMG," *Journal of Neuroscience Methods*, vol. 116, no. 2, pp. 165–177, May 2002.

[64] T. Grujić and A. Kuzmanić, "Denoising of surface EMG signals: A Comparision of Wavelet and Classical Digital Filtering Procedures," *Technology and Health Care*, vol. 12, no. 2, pp. 130–135, 2004.

[65] I. Carreno and M. Vuskovic, “Wavelet Transform Moments for Feature Extraction from Temporal Signals,” *Informatics in Control, Automation and Robotics II*, pp. 235–242, 2007.

[66] A. Kandaswamy, C. S. C. S. Kumar, R. P. Ramanathan, S. Jayaraman, and N. Malmurugan, “Neural classification of lung sounds using wavelet coefficients.,” *Computers in Biology and Medicine*, vol. 34, no. 6, pp. 523–537, Sep. 2004.

[67] M. Nielsen, E. N. Kamavuako, M. M. Andersen, M.-F. Lucas, and D. Farina, “Optimal Wavelets for Biomedical Signal Compression,” *Medical & biological engineering & computing*, vol. 44, no. 7, pp. 561–568, Jul. 2006.

[68] A. O. Andrade, S. Nasuto, P. Kyberd, C. M. Sweeney-Reed, and F. R. Van Kanijn, “EMG signal filtering based on Empirical Mode Decomposition,” *Biomedical Signal Processing and Control*, vol. 1, no. 1, pp. 44–55, Jan. 2006.

[69] A. Phinyomark, P. Phukpattaranont, and C. Limsakul, “Feature reduction and selection for EMG signal classification,” *Expert Systems with Applications*, vol. 39, no. 8, pp. 7420–7431, 2012.

[70] A. Phinyomark, A. Nuidod, P. Phukpattaranont, and C. Limsakul, “Feature Extraction and Reduction of Wavelet Transform Coefficients for EMG Pattern Classification,” *Electronics and Electrical Engineering*, vol. 122, no. 6, pp. 27–32, Jun. 2012.

[71] J. V Basmajian, *Biofeedback: Principles and practice for clinicians*. Baltimore: Williams & Wilkins, 1989.

[72] Y. Blanc and U. Dimanico, “Electrode Placement in Surface Electromyography (sEMG)‘Minimal Crosstalk Area’(MCA),” *Open Rehabilitation Journal*, vol. 4, pp. 110–126, 2010.

[73] G. McLachlan, K. A. Do, and C. Ambroise, *Analyzing Microarray Gene Expression Data*. Wiley, 2005.

[74] R. A. Fisher, “The statistical utilization of multiple measurements,” *Annals of Eugenics*, vol. 8, no. 4, pp. 376–386, Aug. 1938.

[75] D. Novak, M. Mihelj, and M. Munih, “A survey of methods for data fusion and system adaptation using autonomic nervous system responses in physiological computing,” *Interacting with Computers*, vol. 24, no. 3, pp. 154–172, May 2012.

[76] D. Novak, X. Omlin, R. Leins-Hess, and R. Riener, “Predicting Targets of Human Reaching Motions using different Sensing Technologies,” *IEEE Transactions on Biomedical Engineering*, vol. 60, no. 9, pp. 2645–2654, Sep. 2013.

[77] R. G. T. Mello, I. R. Carri, T. T. Da Matta, J. Nadal, and L. F. Oliveira, “Lumbar multifidus and erector spinae electromyograms during back bridge exercise in time and frequency domains,” *Journal of Back and Musculoskeletal Rehabilitation*, vol. 29, no. 1, pp. 123–133, 2016.

[78] S. Rasheed, D. Stashuk, and M. Kamel, “Multi-classification techniques applied to EMG signal decomposition,” in *IEEE International Conference on Systems, Man and Cybernetics*, 2004, vol. 2, pp. 1226–1231.

[79] N. Saito and R. R. Coifman, “Local discriminant bases and their applications,” *Journal of Mathematical Imaging and Vision*, vol. 5, no. 4, pp. 337–358, 1995.

[80] R. R. Coifman and M. V. Wickerhauser, “Entropy-based algorithms for best basis selection,” *IEEE Transactions on Information Theory*, vol. 38, no. 2, pp. 713–718, 1992.

[81] G. Chandrashekar and F. Sahin, “A survey on feature selection methods,” *Computers and Electrical Engineering*, vol. 40, no. 1, pp. 16–28, 2014.

[82] D. H. Wolpert and W. G. Macready, “No free lunch theorems for optimization,” *IEEE Transactions on Evolutionary Computation*, vol. 1, no. 1, pp. 67–82, 1997.

[83] C.-C. Chang and C.-J. Lin, “LIBSVM: A Library for Support Vector Machines,” *ACM Transactions on Intelligent Systems and Technology*, vol. 2, no. 3, pp. 1–27, Apr. 2011.

[84] Y. Aliyari Ghassabeh, F. Rudzicz, and H. A. Moghaddam, “Fast incremental LDA feature extraction,” *Pattern Recognition*, vol. 48, no. 6, pp. 1999–2012, 2015.